KONINKLIJK NEDERLANDS METEOROLOGISCH INSTITUUT

MEDEDELINGEN EN VERHANDELINGEN

76

A. R. RITSEMA AND J. VELDKAMP

FAULT PLANE MECHANISMS OF SOUTHEAST ASIAN EARTHQUAKES

1960

F 4,—

STAATSDRUKKERIJ- EN UITGEVERIJBEDRIJF / 'S-GRAVENHAGE

FAULT PLANE MECHANISMS OF SOUTHEAST ASIAN EARTHQUAKES

KONINKLIJK NEDERLANDS METEOROLOGISCH INSTITUUT
MEDEDELINGEN EN VERHANDELINGEN

76

FAULT PLANE MECHANISMS OF SOUTHEAST ASIAN EARTHQUAKES

A. R. RITSEMA AND J. VELDKAMP

1960

STAATSDRUKKERIJ- EN UITGEVERIJBEDRIJF / 'S-GRAVENHAGE

CONTENTS

Introduction
P and S movements in the focal region 7
The use of S waves in earthquake mechanism studies 8
Method used in plotting the S data 10
Determination of the fault plane mechanism 12

Presentation of the data 13

Analysis of the data 31

Discussion of results
Type of earthquake mechanism 45
Earthquake types 52
Magnitude of the shocks 53
Plunge of the fault motions, dip of the fault planes, and plunge of the B-axes 54
Patterns of B-axes 55
Directions of principal stresses 58
Conclusions 60

Acknowledgements 62

References 63

INTRODUCTION

The data used in this study were for the greater part collected in Djakarta, the former post of the first author, and for the remaining part concerning the shallow earthquakes of the Sunda arc, by the second author in De Bilt. The result for these two groups of shocks have been combined in this paper. The data were reported in reply to questionnaires sent to many seismic stations all over the world. The observations published in the ISS and BCIS bulletins of the shocks in question were also used. Reflected waves have not been used in the present study. Some data on the first motion of reflected waves do occur in the Tables, but these were not considered in the determination of the mechanism in the focus of the earthquakes. Former series of solutions have been published elsewhere (RITSEMA 1957c, VELDKAMP 1959). These solutions have been included in the maps in this paper, but not in the Tables.

P and S movements in the focal region

Let us suppose that the earthquake is caused by a single couple of forces in the x—z plane, acting along the z—axis, the y—z plane being the fault plane

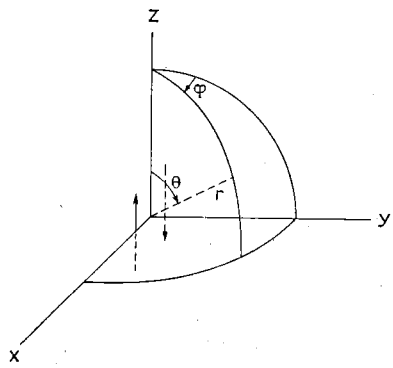

Fig. 1. Planes and axes through the focus of an earthquake.
(y, z) — plane = fault plane.
(x, y) — plane = auxiliary nodal plane for longitudinal waves.
(x, z) — plane = plane of action through the earthquake generating forces.
x-axis = C-axis (MCINTYRE) = normal on fault plane.
y-axis = B-axis (MCINTYRE) = null vector (HODGSON).
z-axis = A-axis (MCINTYRE) = direction of fault motion.

(figure 1). The first author (1957c) has found that such a mechanism can account for the *S* movements in S.E. Asian earthquakes. HONDA (1957) has calculated the displacements produced by a single couple of forces, taking the x-axis as the polar axis of the spherical coordinates r, ϑ and φ. If we transform his formulas to a system with the z-axis as polar axis, the amplitudes of *P* and *S* waves are given by

$$P(r) = \frac{A}{r} \sin \vartheta \cos \vartheta \sin \varphi \qquad (1)$$

$$S(\vartheta) = \frac{B}{r} \sin^2 \vartheta \sin \varphi \qquad (2)$$

In these formulas A and B contain numerical factors, such as the amplitude of the force, the elastic constants and the velocities of longitudinal and transverse waves v_p and v_s.

The formula (1) clearly demonstrates the wellknown fact, that for this type of forces system $P(r)$ becomes zero and changes its sign for $\varphi = o$ (fault plane) and for $\vartheta = \pi/2$ (auxiliary plane), so that the space is divided into four quadrants of compressions and dilatations.

From (2) it follows that the transverse movement $S(\vartheta)$ becomes zero for $\varphi = o$ (fault plane); the movements are equal and opposite on either side of the fault plane. In the quadrants of compressive $P(r)$, the $S(\vartheta)$ movements are directed to the pole of the auxiliary plane, and in the quadrant with dilatations away from it.

The use of S waves in earthquake mechanism studies

The use of S data is based on the assumption that the polarization angle (the angle between the S movements and the plane of incidence of the seismic waves) remains constant along the seismic ray path. If therefore the components SV and SH of the S movement inside the earth (SV = movement in the plane of incidence, SH = movement perpendicular to it) can be determined from the movements recorded at the surface of the earth, they can be used for reconstructing the S movement in the focal region.

Two horizontal components of the ground movement can be read in the seismograms, viz. u in the direction of the epicentre and v perpendicular to this direction; it is not necessary to consider the vertical component w. An SH wave incident at the surface of the earth is reflected as a transverse wave with the same direction of polarization and with the same amplitude. For all angles of incidence

$$v = 2\ SH \tag{3}$$

For the SV wave there is the complication that u and w not only depend on the angle of incidence β but also on Poisson's ratio σ; moreover for $\sin\beta > v_s/v_p$, the angle of refraction α of the reflected longitudinal wave becomes imaginary. Taking $\sigma = 1/4$, the ratio between the horizontal component u and the incident amplitude SV is for $\alpha < \pi/2$

$$\frac{u}{SV} = \frac{6\cos\beta\cos 2\beta}{3\cos^2 2\beta + \sin 2\alpha \sin 2\beta} \tag{4}$$

The reflected longitudinal wave vanishes for $\sin\alpha > 1$ and the movement in the surface becomes elliptic. The ratio between u and SV is then

$$\frac{u}{SV} = \frac{6\cos\beta\cos 2\beta}{\sqrt{9\cos^4 2\beta + 12\sin^2\beta\,(3\sin^2\beta - 1)\sin^2 2\beta}}\ e^{-i\varphi} \tag{5}$$

where

$$\varphi = arc\ \mathrm{tg}\ \frac{2\sin\beta\sin 2\beta.\sqrt{3\sin^2\beta - 1}}{\sqrt{3}.\cos^2 2\beta} \tag{6}$$

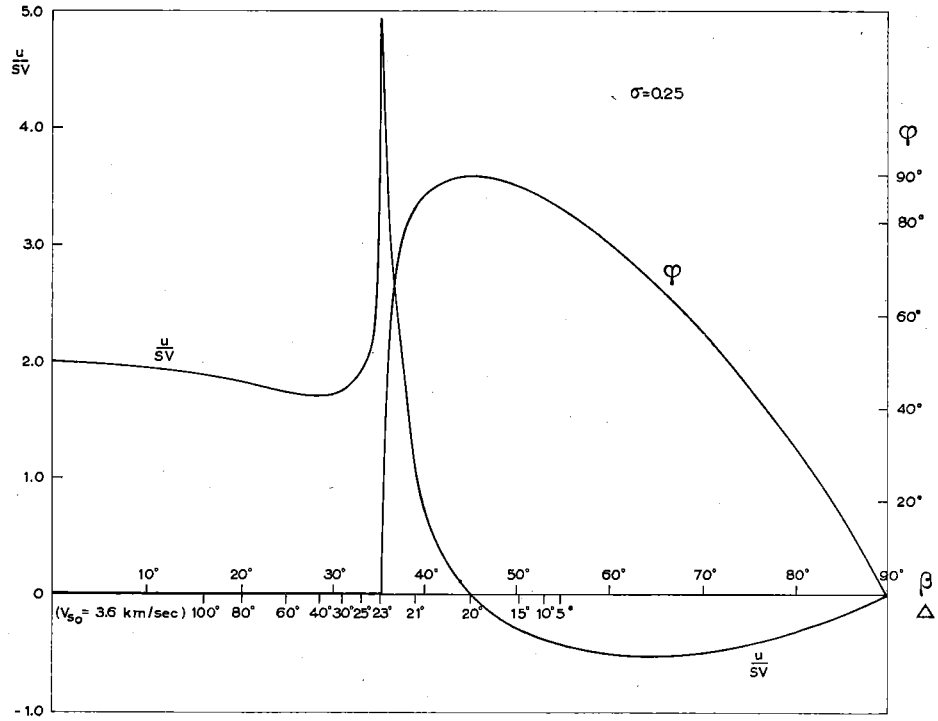

Fig. 2. The ratio between the horizontal component of the ground motion in the plane of incidence and the incident amplitude of the SV wave (u/SV), and the phase angle φ, as a function of the angle of incidence β and the epicentral distance $\triangle$ (for Poisson's ratio $\sigma = 0.25$ and velocity of transverse waves just below the surface $v_s = 3.6$ km/sec).

In figure 2 the value u/SV is given as a function of the angle of incidence β; the phase difference φ between u and SV (see also Table I) is included in the figure.

For practical application the angle of incidence must be converted into the epicentral distance $\triangle$ by means of

$$\sin \beta = v_s \frac{dt}{d\triangle} \tag{7}$$

A (β, $\triangle$)-graph has been drawn (RITSEMA 1958) using the travel time tables of Jeffreys and Bullen and assuming a velocity of the transverse wave at the surface of the earth of $v_s = 3.6$ km/sec. Figure 2 has been completed with values of $\triangle$ valid for superficial earthquakes.

We see from figure 2 and Table I, that for values of β smaller than 34° or $\triangle$ larger than 24°, u is between 1.8 SV ans 2.0 SV so that the ratio u/v is practically

TABLE I

Values of u/SV and φ as a function of α and β (using σ = 0,25). Column 6 shows β as a function of △ for superficial earthquakes and v_s = 3.6 km/sec.

α	β	u/SV	φ	△	β
0	0	2.000	—	100°	16°
10°	5° 45′	1.984	—	90	17° 15′
20	11 23	1.937	—	80	20
30	16 47	1.868	—	70	22 15
40	21 47	1.791	—	60	24 45
50	26 15	1.730	—	50	26 30
60	30	1.732	—	40	28 30
70	32 52	1.895	—	30	31
80	34 39	2.511	—	25	33
90°	35 16	4.899	0 00	24	34
	40	0.741	85° 12′	23	35
	45	0.000	90	22	36
	50	−0.294	87 44	21	39
	60	−0.500	75 31	20	45
	70	−0.489	56 46	15	50 15
	80	−0.316	31° 20′	10	53
	90°	0.000	0 00	5°	54° 45′

the same as *SV/SH*. For values of β larger than 35° or for epicentral distances smaller than 23° there is a phase difference between *u* and *v* so that no simple relation exists between *u/v* and *SV/SH*.

For other values of Poisson's ratio σ these critical epicentral distances are changed to a very small degree only. For σ = 0.24 (a normal value for the continental crust) the maximum in *u/SV* is found at β = 36° and △ = 22°; for σ = 0.273 at β = 34° and △ = 24°.

The △-values of figure 2 are slightly displaced by using other values of the velocity of transverse waves. For v_s = 3.15 km/sec (an average value for sedimentary rocks) the maximum in *u/SV* occurs at △ = 19°, and for △ > 20° *u/v* is about equal to *SV/SH*. For oceanic stations a value of 3.9 km/sec may be taken for the velocity of the upper crust; in this case the maximum of the curve corresponds to a △ of 26°, and for △ > 29° is *u/v* about equal to *SV/SH*.

Summarizing we may say that for stations situated on a normal continental crust *SV/SH* can be replaced by *u/v* if △ > 25°; for oceanic stations this must be △ > 30°. The influence of the depth of focus is negligible at these distances.

Method used in plotting the S data

The first amplitude of the S wave is read in the seismograms in two horizontal components. Only clear *S* waves can be used, preferably recorded by two horizontal seismographs with the same magnification curve.

The azimuth of the epicentre as seen in the station is determined from the known positions of epicentre and station (WILLMORE and HODGSON, 1955). The first S movement is resolved into the components u and v, and if necessary u is corrected for the data of table I and figure 2, in order to give the actual ratio SV/SH and the polarization angle of the incident wave.

Taking into account that the S readings are never absolutely accurate, no correction is necessary for stations with $\triangle > 25°$ (continental crust) or $\triangle > 30°$ (oceanic crust).

Now the polarization angle of the S wave must be projected along the seismic ray from the station upon a small sphere around the focus of the earthquake. This is done by means of

$$\sin i = \frac{cr_o}{r}\frac{dt}{d\triangle} \tag{8}$$

where c is the seismic velocity in the hypocentre, r_o is the earth's radius, r is the distance from the focus to the centre of the earth, and i is the angle of incidence of the seismic ray in the focus.

The $(i, \triangle)$-curves calculated after (8) have been published earlier (RITSEMA, 1958). The seismic projection of the station on the lower half of this sphere is drawn in a stereographic diagram (see figure 3). It is clear that a motion of SH to the left or to the right as seen from the epicentre remains the same in the stereographic projection. As for SV, a motion which in the station was directed towards the epicentre must be drawn as a movement pointing away from the centre of the diagram, and a motion in the station directed away from the epicentre must be drawn as a movement pointing to the centre of the diagram, owing to the curvature of the ray path. T means a motion towards the epicentre, and F away from, R means to the right and L to the left. The S vector resultant from SH and SV gives the direction of the first S wave in the focal region (see also RITSEMA, 1957b, 1957c).

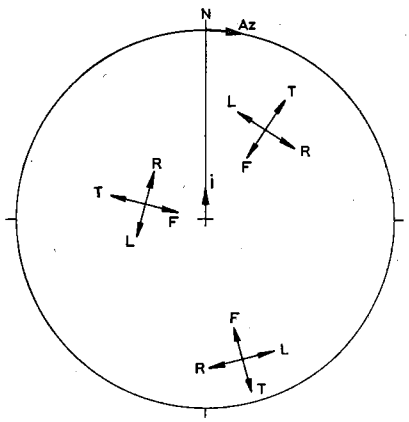

Fig. 3. The plotting of SH (R or L) and SV (T or F) in the stereographic net.

The S vectors as determined in different stations should point uniformly to one of the poles of the two nodal planes for P waves, viz. to the pole of the auxiliary plane, if a single couple of forces is supposed in the focus (fig. 4). In practice the S vectors often do not point to one pole, which for an important part will be caused by the small accuracy with which S onsets can be read in the seismograms.

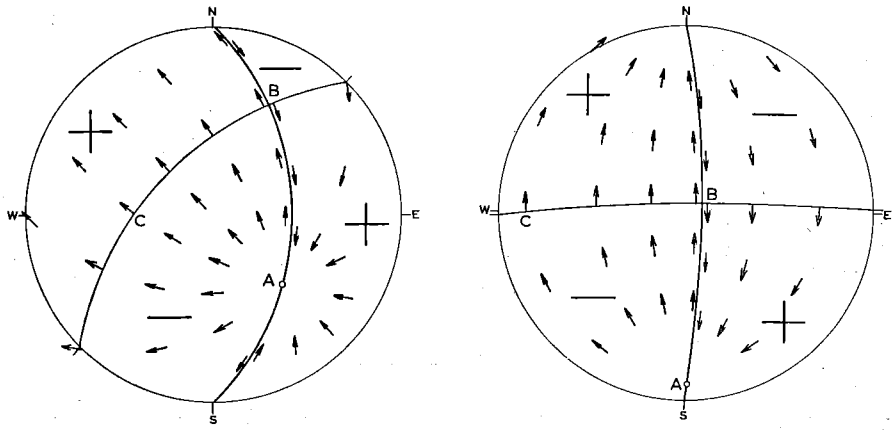

Fig. 4. Stereographic projection of the direction of first S motion around the focus in the single couple model.

Determination of the fault plane mechanism

If a sufficient number of *P* data is available, it will in general be possible to draw the nodal planes between the compressions (*C*) and dilatations (*D*) as great circles in the diagram.

The circles must intersect perpendicularly on account of the orthogonality of the nodal planes. The *S* vectors must follow great circles through the pole of the auxiliary plane in this sense, that in the compressive sector they must point towards this pole and in the dilatative sector away from it. It may in many cases be possible to distinguish between the fault plane and the auxiliary plane by the better fit of the *S* data for one of the two, even if only a few *S* data are available.

When doing this we must take into account that one possible error in reading the seismograms is that the time of the first movement may be taken half a period, or even one and a half, too late. This means that the computed first motion may be just opposite to the real one. Therefore, deviations of the *S* vectors over 180° from the expected direction are not considered as serious inconsistencies.

Finally it is once again stressed that the solutions given in this publication as well as in the preceding ones, represent the best agreement of the data. This means that these solutions are not absolutely certain, so that the conclusions reached in this study should be considered with some reserve.

PRESENTATION OF THE DATA

The earthquakes for which a solution has been obtained are collected in Table III. Together with those of Table II, giving the earthquakes for which no solution could be reached owing to too few or too conflicting data, this is the total material on which the investigation was based.

Table IV gives the *P* and *PKP* data for the different earthquakes. As the earthquakes are all from S.E. Asia, the more distant recording stations are always situated in the same general direction from the focus. This is the reason that the stations in Table IV, V and VI have been arranged in continents. This facilitates the plotting of the data in the diagrams, and also the tracing back of a station from the diagram to the Table.

D means a dilatational *P* wave, C a compressional *P* wave, D′ stands for a dilatational *PKP* wave, C′ for a compressional *PKP* wave. The data in italics are inconsistent with the solution reached, the others are consistent.

In Table V a few data on reflected longitudinal waves for some of the earthquakes are collected. The nomenclature used is intended as a direct indication on the character of the wave.

PP waves are given as CD or DC which shows that we assume that a longitudinal wave changes its phase by reflection at the earth surface. For values of σ larger than 0.20 this is true for angles of incidence $\alpha < 50°$, and $\alpha > 84°$, and therefore for epicentral distances of the PP wave larger than 40° and smaller than 4° (INGRAM and HODGSON, 1956, and HODGSON and ADAMS, 1958). CD means that the wave left the focus as a compression and arrived in the station as a dilatation, and vice versa with DC. The pP waves are given as cD and dC respectively, and in the same way cD′ and dC′ are representations of pPKP waves.

PcP waves are given as CC and DD respectively, indicating that we assume that no change of phase occurs at reflection against the earth core. This is true

TABLE II *Earthquakes for which the data were too few or too conflicting to permit a solution*

Date	Time	Epicentre	Depth
1930, Mar. 26,	07h 12m 08s	7¾° S 125½° E	s
1931, Sept. 25,	05 59 52	5 S 102½ E	s
1933, May 16,	01 12 31	6½ N 96½ E	s
1934, May 1,	07 04 56	3½ N 97½ E	0.01 R
1935, June 22,	15 48 36	6 S 120½ E	s
Aug. 3,	01 10 09	5 N 96¼ E	s
1938, July 29,	13 06 45	0 100 E	0.01 R
1947, May 6,	20 30 32	6½ S 148¾ E	s
1951, Jan. 8,	21 39 29	5 S 150 E	s

TABLE III *Earthquakes for which a solution has been obtained*

No.	Date	Time	Epicentre	Depth	Magn.
1	1934, Apr. 10,	$10^h\ 23^m\ 02^s$	7 °S 116 °E	shallow	$6\frac{3}{4}$
2	1937, Sept. 27,	08 55 20	$8\frac{3}{4}$ S $110\frac{3}{4}$ E	0.005 R	7.2
3	1938, Feb. 1,	19 04 21	5 S $131\frac{1}{2}$ E	s	8.2
4	1940, Mar. 21,	13 52 51	$10\frac{1}{2}$ S $107\frac{1}{2}$ E	s	$6\frac{3}{4}$
5	Mar. 28,	15 48 50	$14\frac{1}{4}$ N $120\frac{1}{2}$ E	0.02 R	$6\frac{3}{4}$
6	1941, June 26,	11 52 00	$12\frac{1}{2}$ N $92\frac{1}{2}$ E	0.005 R	8.1
7	1942, Apr. 8,	15 40 24	$13\frac{1}{4}$ N $120\frac{1}{2}$ E	s	7.7
8	July 29,	22 49 13	$2\frac{3}{4}$ S $127\frac{3}{4}$ E	s	7.0
9	1943, Apr. 1,	14 18 12	$6\frac{1}{2}$ S 106 E	s	7.0
10	May 25,	23 07 36	$7\frac{1}{2}$ N $127\frac{1}{2}$ E	s	7.9
11	Nov. 6,	08 31 34	$5\frac{3}{4}$ S 134 E	s	7.6
12	1944, Mar. 31,	02 51 44	$5\frac{1}{2}$ S 131 E	0.005 R	7.0
13	Apr. 26,	01 54 11	$\frac{3}{4}$ S $133\frac{1}{2}$ E	s	7.2
14	Apr. 27,	14 38 03	1 S 133 E	s	7.4
15	Nov. 15,	20 46 57	$4\frac{1}{2}$ N $127\frac{1}{2}$ E	s	7.2
16	1945, Oct. 16,	16 03 02	0 $123\frac{3}{4}$ E	0.005 R	7.1
17	1946, Jan. 17,	09 39 36	$6\frac{1}{4}$ S $147\frac{3}{4}$ E	0.01 R	7.2
18	1947, May 27,	05 58 52	$1\frac{3}{4}$ S $135\frac{1}{2}$ E	0.01 R	$7\frac{1}{4}$
19	1948, Jan. 24,	17 46 43	11 N 122 E	s	8.2
20	Mar. 1,	01 12 24	3 S $127\frac{1}{4}$ E	s	7.5
21	1949, Mar. 27,	06 34 01	$3\frac{1}{4}$ N $127\frac{3}{4}$ E	s	7.0
22	Apr. 23,	11 15 35	$7\frac{1}{2}$ S $120\frac{3}{4}$ E	0.00 R	7.1
23	June 24,	22 38 36	$6\frac{1}{4}$ S $105\frac{3}{4}$ E	0.005 R	7
24	Dec. 29,	03 03 54	18 N 121 E	s	7.2
25	1950, Sep. 19,	20 29 48	2 S $138\frac{1}{2}$ E	s	6.9
26	Oct. 8,	03 23 09	4 S $128\frac{1}{2}$ E	s	7.6
27	Nov. 2,	15 27 56	$7\frac{1}{2}$ S 129 E	0.03 R	7.5
28	Nov. 8,	02 18 12	$9\frac{3}{4}$ S $159\frac{1}{2}$ E	s	$7\frac{1}{4}$
29	1951, Nov. 29,	04 45 43	$\frac{1}{2}$ N $120\frac{1}{2}$ E	s	$6\frac{1}{2}$
30	1952, May 8,	21 10 40	$2\frac{1}{2}$ N 127 E	s	$6\frac{3}{4}$
31	Nov. 6,	19 47 20	5 S $145\frac{1}{2}$ E	s	7.3
32	Nov. 28,	21 01 27	$6\frac{1}{2}$ S $155\frac{1}{2}$ E	0.01 R	$6\frac{3}{4}$
33	Dec. 24,	18 39 38	$5\frac{1}{2}$ S 152 E	s	7
34	1953, Apr. 23,	16 24 17	4 S 154 E	s	7.6
35	1954, July 2,	02 45 09	13 N 124 E	s	7
36	1955, Mar. 31,	18 17 12	8 N 124 E	0.005 R	$7\frac{1}{2}$
37	May 17,	14 49 49	$6\frac{1}{2}$ N 94 E	s	$7\frac{1}{4}$
38	May 29,	15 34 04	10 S $110\frac{1}{2}$ E	s	$6\frac{1}{2}$
39	Sep. 15,	12 30 27	5 S $134\frac{1}{2}$ E	s	$6\frac{3}{4}$
40	1956, Feb. 12,	11 49 20	19 N $119\frac{1}{2}$ E	s	$6\frac{3}{4}$
41	May 22,	12 36 12	4 S $152\frac{1}{2}$ E	0.08 R	$6\frac{3}{4}$
42	1957, Feb. 10,	22 32 15	10 N 126 E	s	$6\frac{3}{4}$
43	Feb. 10,	22 50 52	$10\frac{1}{2}$ N $126\frac{1}{2}$ E	s	$6\frac{3}{4}$
44	Feb. 11,	01 14 44	10 N 126 E	s	$6\frac{1}{2}$
45	Mar. 23,	05 12 31	$5\frac{1}{2}$ S 131 E	0.01 R	7
46	Apr. 16,	04 04 04	$4\frac{1}{2}$ S $107\frac{1}{2}$ E	0.09 R	$7\frac{1}{2}$
47	May 2,	21 36 25	$7\frac{1}{2}$ S 120 E	0.09 R	$6\frac{3}{4}$
48	June 22,	23 50 23	$1\frac{1}{2}$ S 137 E	s	7.2

for a value of ϱ_1/ϱ_2 at the core mantle boundary of 1.7 (Bullen's Model I) for epicentral distances smaller than 88°; for a density ratio of 1.6 (Bullen's model II) no phase change occurs for epicentral distances between 9° and 87° (BÅTH, 1957).

Table VI comprises the S data. These are given as the azimuth in which the first movement of S takes place at the station. The first ground motion is calculated from the amplitudes in NS and EW components. The azimuth is always given as the direction N through E.

Bold type figures are consistent with the solution given, normal type figures are consistent if we assume that not the first motion was read in the seismograms but the motion which occured (n + $\frac{1}{2}$) period later (consistent $\pm$ 180°); italics are inconsistent directions.

Table VII gives the numbers of consistent and inconsistent data of the different wave types for each individual earthquake. There are three columns for the S wave, the first one giving the numbers of consistent and inconsistent data for the solution obtained, the second one giving these figures for the alternative solution in which the original auxiliary nodal plane is supposed to be the fault plane and the pole of the original fault plane to be the direction of the fault movement. This has been done to give an insight into the reliability of the choice that has been made between these two. The third column gives the figures that are valid for the solution, supposing that HONDA's model of earthquake mechanism is acting.

Table VIII summarizes the solutions reached in terms of the direction of fault movement (azimuth and plunge), of the normal to the fault plane (azimuth and plunge), of the B-axis (azimuth and plunge), and of the fault type.

Two of these data with the fault type are sufficient for a complete insight into the motions in the focus. The earthquake type is given as follows: L = left-handed transcurrent (sinistral), R = right-handed transcurrent (dextral), P = reverse (or thrust) and T = normal. All types of block motion can be described as a combination of L or R with P or T. This has been done so that the first character is always the dominating one of the two.

Tables VIIa, VIIIa contain the results of earthquakes which occurred on and near the isle of Sumatra. A preliminary report on these shocks has already been published (VELDKAMP, 1959). For some of these earthquakes the solutions presented here must be considered as improved compared with the preliminary report. Some other solutions have been added.

Figures 5—11 show examples of fault plane solutions for some of the investigated earthquakes. Figures 7 and 11 give solutions which are considered as good, figures 8, 9 and 10 are fair solutions, whereas figures 5 and 6 are examples of solutions which can only be called poor. Open circles represent dilatations of first P movements, black dots are compressions. The small arrows are *S* vectors. The fault movement is indicated by the long arrow, which gives the motion direction of the upper block.

TABLE IV

P and PKP data on the earthquakes for

	1	2	3	4	5	6	7	8	9	10	11	12	13	14	15	16	17	18	19	20	21	22	23	24
Australia, S. Pacific																								
Apia											D											C		
Auckland						C								*D*			C	D	C					D
Brisbane											D	D		C	C									
Christchurch						C	*C*																	
Melbourne	C	D	D	D							D									C			D	
Noumea																								
Perth	C	D	D	D	C	C	*C*				D	D	*D*	D	C	D	C	D		C	C	D		C
Riverview		D	D	D	D	*D*	D	D	C	C	D	D	C	C	C	C	C	D	C	C	C	C	C	C
Sydney														C										
Wellington		C			D	C	D	D		D	D	D	D	*D*	C	C		D	*D*	C	*D*		C	D
Asia																								
Amboina					C	C																		
Bandung																								C
Bombay	C	C	C	*C*			*C*	D	C		C	C								C		C	C	
Calcutta						D	D	D				C	D						*D*	D	C			
Chiufeng	C																							
Dehra Dun						D																		
Djakarta		D	C	C	D	C	C	D	C	D	C	C	C	D	C	D			*C*	C	D	D	C	C
Fukuoka																								
Heizyo			D																					
Hongkong		D	D																					
Hyderabad	C	C	C	D		D	D	D	C	D	C	C	C	D	C	C	D	C	C	C	C	C	C	D
Irkutsk		C	D					D				C								C			C	
Jerusalem																								
Kobe					C	C	C			C								C						
Kodaikanal	C		C	D	D		D	D	C		C	*D*								C		C	C	
Ksara		*D*	C	D	C															C		C	C	
Lembang																								
Manila	C	C		C	C	C																		
Matsushiro																								
Medan					D	C																		
Miyazaki										C														
Nangking	*D*																							
New Delhi					D		D	D	D				D	D	D	D							C	
Oita																								
Hiroshima																								
Osaka																								
Quetta																								
Sapporo					C	D	C			C							D							
Stalinabad																								
Tashkent	C	*C*						D	C			C								C				

which a solution have been obtained

25	26	27	28	29	30	31	32	33	34	35	36	37	38	39	40	41	42	43	44	45	46	47	48	
																								Australia, S. Pacific
																								Apia
D																							D	Auckland
C		D	D																					Brisbane
											C					D								Christchurch
																	D	D	D	C	D	D	C	Melbourne
											C			D	C	D								Noumea
D	D	D	C		C	D	D		D	C	C	*D*	C				D			C	C		C	Perth
D	*C*	D	D	C	C	D	D	C	D	*D*	*D*	C	*C*	D	D	D	C	C	C	D	D	D	C	Riverview
																								Sydney
D	D	D	D	D	*D*		D				C			*C*		D				D	D	D	C	Wellington
																								Asia
																								Amboina
D				C		C	D		D	D	*C*	C			*C*	C	*C*	*C*	D	C	*C*	*C*	D	Bandung
	C	C											C											Bombay
																								Calcutta
																								Chiufeng
																								Dehra Dun
D	C	C	D	C	D	C	D	D	*C*	D	D	C	D	C	D	C	D	*C*	D	C	D	D	D	Djakarta
		C								C	D	D			D									Fukuoka
																								Heizyo
						C	C		C	C	C	D			C	C	*D*	*D*	C	C	C	C		Hongkong
D	C	C		C	D	C			D	D	D	C			D	C	C	C	C	C	D	C	D	Hyderabad
	C	C											C	D										Irkutsk
															C		*D*	C			*C*			Jerusalem
											C									D	C		*D*	Kobe
	C																							Kodaikanal
		C													D									Ksara
										D	*C*	C			D	C	D	*C*		C	D	D		Lembang
											C		C	C			C							Manila
										D		D	C	D	D					D	C			Matsushiro
																D	D	D	C		D	C	D	Medan
	D	C																						Miyazaki
C	C	C	*C*																					Nangking
																								New Delhi
	C																	D						Oita
																		D						Hiroshima
										D										D	C			Osaka
					D	*D*	D	D		C	D	C		D	D	C	C	C	C	C	D	D	D	Quetta
	C		D		C		C		D	C	D	D			D					D				Sapporo
													D	D										Stalinabad
		C											C	D										Tashkent

TABLE IV (continued) *P and PKP data on the earthquakes for*

	1	2	3	4	5	6	7	8	9	10	11	12	13	14	15	16	17	18	19	20	21	22	23	24
Tokyo		C	D					D			C									D		C		
Tooyoka		*D*																						
Zinsen		C	D																					
Zi Ka Wei					*D*																			
Akita																								
Kumagaya																								
Maebasi																								
Miyako																								
Morioka																								
Sumoto																								
Africa																								
Alger																								
Astrida																								
Grahamstown																								
Helwan				D	C	D	C	D		C			C					C	C	C	C		C	C
Hermanus																								
Kimberley																								
Lwiro																								
Pietermaritzburg																								
Pretoria																								
Tamanrasset																					D′		D	
Tananarive	D	C				C	C	*C*	C	C			C	C	C	C			D	C	D	D	D	C
Uvira																								
Europe																								
Aberdeen						D	*D*			*D*									*D*					
Alicante						D	C			C			*D′*	*C′*	*C′*	*D*	D′	D′	D′		D′			*D*
Almeria						D	C			*D*			*D′*	*C′*	D′	C	D′	D′			*C′*			
Athena																								
Béograd		D														C							C	C
Bergen																								*D*
Bologna																								C
Bucarest			D			D																		
Chur										C									C					C
Clermont F.						D	*D*																	
De Bilt					C	D	C	D		C			*C*	C		C		D′	C		*D*		*D*	C
Dublin																								
Erevan																								
Firenze										*D*	*C′*													C
Granada						D				*C′*			*D′*	*C′*	D′		D′	D′	D′	*D*	D′		*D′*	C, *C′*
Hamburg			*C*		C																			
Helsinki																								C

which a solution have been obtained

25	26	27	28	29	30	31	32	33	34	35	36	37	38	39	40	41	42	43	44	45	46	47	48	
	C	D																						Tokyo
																								Tooyoka
																								Zinsen
	D																							Zi Ka Wei
	D																							Akita
	D																							Kumagaya
		C																						Maebasi
	C	C																						Miyako
	C																							Morioka
																								Sumoto
																								Africa
	D′																						D′	Alger
												D												Astrida
		C				C						D			D	*D*′	C	C			D			Grahamstown
												C									D	D		Helwan
												C				C′					*C*			Hermanus
												D			D						D			Kimberley
																					D			Lwiro
												D			D						*C*			Pietermaritzburg
C′	D′							D′				D	C	D	*C*	C′	D	D	D	*C*′	D	D′	D′	Pretoria
	D	D				C					D						*C*							Tamanrasset
																								Tananarive
																	C							Uvira
																								Europe
										C	D							C						Aberdeen
C′			*C*′		*C*′	C′	D′	C′		C′	C′	C			*C*			C′		*C*′	*C*	*C*′	*C*′	Alicante
C′			D′				D′	C′	*C*′	C		C			*C*	C′				*C*′	D			Almeria
									C′	C	C	C									D			Athena
	C		D′							C	*D*	C					C		*D*		D			Béograd
												D												Bergen
																								Bologna
																								Bucarest
		D																						Chur
																					D			Clermont F.
	D									C	D	C			D						D			De Bilt
D′									D′		*C*	*D*			D	C′						*C*′		Dublin
													C	D										Erevan
							D′				C										D			Firenze
D′	*C*′	D′	D′		D′	C′	D′	C′			C, *D*′	*D*				C′					D	D′		Granada
																								Hamburg
																								Helsinki

TABLE IV (continued) *P and PKP data on the earthquakes for*

	1	2	3	4	5	6	7	8	9	10	11	12	13	14	15	16	17	18	19	20	21	22	23	24
Kew			D			D	C	D			D		D	*D*						C			C	
Kiruna																								
Kirovabad																								
København		C	*C*	C	C	D	C			C			D	C	D	C			C	*D*			C	C
Lisboa						D				D′	D′		C′	*D*′			D′			C′				
Malaga													C′	C′	D′	*D*′		*C*′						
Messina																								*D*
Makhachkala																								
Monaco																								
Moscow		C				D						C							C		C	C	C	C
Paris																			C					
Pavia																								
Potsdam						D	C	D											C					C
Praha						D	C			*D*			D, C′	C′					C					C
Pulkovo																								
Reggio Calabria																								
Relizana																								
Roma				D	C														C	C			C	C
Simferopol																								
Skalstugan																								
Strasbourg			D			D																		C
Stuttgart						D	C			C										C	C		C	
Tblisi								D												C				
Toledo													C′											
Trieste			D		C															C				
Uccle							C			C						C				C				
Uppsala						D				C									C	C				C
Warszawa				D	C	D	C												C	C				
Witteveen																								
Yalta																							C	
Zagreb																								C
Zürich						D	C												C		C			C
North America																								
Arcata																								
Boulder City																								
Berkeley													D						C.		*C*	*D*′	C′	D
Bozeman																								
Brébeuf																								
Butte																								
Cleveland																								
College																								
Columbia																								
Corvallis																								
Eureka																								

which a solution have been obtained

25	26	27	28	29	30	31	32	33	34	35	36	37	38	39	40	41	42	43	44	45	46	47	48	
	D	C											D								D			Kew
				D			C′	C′		D	D	C		C	D		C	C			D	D	D	Kiruna
													C											Kirovabad
	D	C	D′				D′			C	C	C			D	D′	D		D		D		C	København
	C′	D′	C′									C										D′	C′	Lisboa
D′	C′	D′	C′				C′	C′			D′	C				D′					C	C′		Malaga
												D								D′				Messina
													D											Makhachkala
																					D			Monaco
	D	D			C	C			C		C	C	D	D	C	C, C′	C	C	C	D	D	D	C	Moscow
																								Paris
		C								C		D												Pavia
	D	C																						Potsdam
		C										C			D						D			Praha
													D											Pulkovo
																					D			Reggio Calabria
																					D			Relizana
		C	D′								C	C	D		D									Roma
													C											Simferopol
																C′	C			D	D	C		Skalstugan
		C																			D			Strasbourg
		C																		D′	D			Stuttgart
													C	D										Tblisi
																								Toledo
								C′				C						C			D			Trieste
																								Uccle
								C′		C	D	C			D		C	C	C	D	D		C	Uppsala
																					D			Warszawa
							D′		D′	C	D	C			D	D′	D				D			Witteveen
													C											Yalta
												D												Zagreb
		C									C	C												Zürich
																								North America
C																								Arcata
																					D′			Boulder City
C	C	C	C	C′		D		C		C	C	C′		D						D	D′	D′		Berkeley
											C										D′			Bozeman
																					D′			Brébeuf
																				D	C′			Butte
	D′	D′												C′										Cleveland
										D	C									D	C		C	College
																					D′			Columbia
																					D′			Corvallis
																		C						Eureka

TABLE IV (concluded) *P and PKP data on the earthquakes for*

	1	2	3	4	5	6	7	8	9	10	11	12	13	14	15	16	17	18	19	20	21	22	23	24
Fayetteville																								
Fordham				C′	*D′*																			
Fresno																							*D′*	
Georgetown	C′																							
Harvard																								
Honolulu																								
Lick																							C′	
Mineral																							C′	D
Morgantown																								
Mt. Hamilton																								
Mt. Wilson																	C							
Nelson																								
Oak Ridge		D′																			D′			
Ottawa																								
Palisades																								
Pasadena				D′				D												C		C′		D
Pennsylvania																								
Rapid City																								
Reno																								
Riverside				D′																				
Salt Lake City																								
Seattle																								
Shasta																								
Scoresby Sund					C	*C*	*D*			D									C					*D*
Sta. Clara																								D
St. Louis		C′						*C′*															C′	
Temiskaming																				C′				
Tucson																								
Ukiah																								
Vermont		C′																						
Victoria																								D
Ville Marie																				C′				
Weston		D′	C′															D′						
S. & C. America																								
Antigua																								
La Paz		D′	C′	D′	C′		C′	D′		*C′*			C′			C′	D′			C′	C′	C′		C′
Merida																								
Montezuma																								
San Juan																								
Sta. Lucia																								
Tacubaya																								
Trinidad																								

which a solution have been obtained

25	26	27	28	29	30	31	32	33	34	35	36	37	38	39	40	41	42	43	44	45	46	47	48	
													D′				D′	D′	D′	C′				Fayetteville
																								Fordham
C	C	D	*D*																					Fresno
																								Georgetown
											C													Harvard
																							D	Honolulu
C		D	C																					Lick
			C	D′	D		C	C			*D*				D	C	C			D		D′		Mineral
											C′	D′					C′					D′		Morgantown
			C							D	*D*	*C′*		D	*C*						D′		Mt. Hamilton
																								Mt. Wilson
										C														Nelson
																								Oak Ridge
																								Ottawa
								D′		D′	C						D′	D′	D′	D′	D′	D′		Palisades
	C		C	D′																		D′		Pasadena
											C′	*C′*								D′	D′		D′	Pennsylvania
																					C′			Rapid City
	C	D	C	*C′*	D	D	C	C			C	*C′*			D					D	D′	D′		Reno
			C																					Riverside
																				D				Salt Lake City
D		D	*D*			D															D′			Seattle
										D	C	*C′*			D					D	D′	D′		Shasta
							D′		D	C	D	D			D		C	D			D,D′			Scoresby Sund
	C′	D′											D′							C′				Sta. Clara
																								St. Louis
												D′												Temiskaming
																					D′			Tucson
																								Ukiah
																								Vermont
																								Victoria
						C′		D′	C′															Ville Marie
																		D′			D′	D′	D′	Weston
																								S. & C. America
																					D′			Antigua
	C′	C′		C′	C′					D′				D′	D′	D′					D′			La Paz
												D′								D′				Merida
										C′		C′	C′											Montezuma
											C′	D′										D′	C′	San Juan
																					D′			Sta. Lucia
												D′									D′			Tacubaya
																						D′		Trinidad

TABLE V *Reflected longitud*

Earthquake number →	2	12	13	14	16	21	22	23	24	25	28	30	32
Perth					DC						CD		
Djakarta													cD
Béograd							CD			DC			
Bucarest				DC									
Firenze													
Granada		CD											
Lisboa		*DC*						*DC*	*CD*				
Malaga						*DC*			DC			CD	
Makhachkala													
Monaco													
Moscow						cD						cD	
Pavia													
Potsdam							*DC*						
Stuttgart	DC						CD						
Uccle			DC										
Cleveland											CD		
Corvallis													
Harvard												DC	
Mt. Hamilton													
Shasta													
Sta. Clara													
Merida													
Riverview							cD						
Sumoto							DC						
Tananarive							DC [3]						
Aberdeen							CD						
Leipzig							CD						
Roma							*DC*						

[1]) also CD [2]) also CD and dC′ [3]) also dC

Remarks:

DC, dC = PP, pP dilatation from the focus, compression in the station.

CD, cD = PP, pP compression from the focus, dilatation in the station.

Italics are inconsistent.

inal wave data

35	36	37	38	39	41	42	44	45	46	47	48	Earthquake ← number
												Perth
			CD									Djakarta
												Béograd
												Bucarest
									cD			Firenze
CD				*CD*			CD			DC		Granada
												Lisboa
				CD								Malaga
												Makhachkala
									DC			Monaco
	cD	cD [1])			*cD* [2])	CD			dC	*cD*	*DC*	Moscow
								CD				Pavia
												Potsdam
												Stuttgart
												Uccle
												Cleveland
									cD'			Corvallis
												Harvard
DC												Mt. Hamilton
DC												Shasta
								DC				Sta. Clara
								DC				Merida
												Riverview
												Sumoto
												Tananarive
												Aberdeen
												Leipzig
												Roma

TABLE VII *Numbers of consistent*(c) *and inconsistent* (i) *data of the earthquakes for which a solution has been obtained*

Earthquake number	P		PKP		PP		S			S for alternative solution			S for Honda's solution		
	c	i	c	i	c	i	c	c±180°	i	c	c±180°	i	c	c±180°	i
1	9	1	1	0			2	3	0	0	0	5	0	1	4
2	15	4	5	0	1	0	5	3	0	0	0	8	2	2	4
3	17	2	2	0			2	1	2	1	1	3	2	1	2
4	11	1	4	0			0	3	0	0	0	3	0	1	2
5	20	1	1	1			2	3	3	3	1	4	0	3	5
6	33	2	0	0			7	2	2						
7	22	6	1	0			5	1	2	0	2	6	1	3	4
8	17	1	1	1			3	1	2						
9	8	0	0	0			3	0	1	0	1	3	3	1	0
10	17	4	1	2			1	3	2	0	1	5	1	2	3
11	12	0	1	1			3	3	0	0	1	5	0	0	6
12	11	1	0	0	1	1	5	1	1	0	1	6	3	1	3
13	12	2	5	3	1	0	1	1	1	1	0	2	0	0	3
14	10	3	5	1	1	0	2	1	1	1	0	3	2	1	1
15	9	0	3	1			2	2	1						
16	12	1	1	1	1	0	1	0	0	0	0	1	0	0	1
17	6	0	5	0			1	0	1	1	0	1	1	0	1
18	7	0	5	1			2	0	0	0	1	1	0	0	2
19	18	4	2	0			2	2	2	1	2	3	2	2	2
20	24	2	4	0			3	2	1	1	0	5	2	1	3
21	10	3	5	1	1	1	2	2	2	1	1	4	2	1	3
22	11	0	6	3	2	1	3	1	1						
23	22	1	5	2	0	1	5	2	3	0	3	7	4	1	5
24	30	3	2	0	1	1	1	2	2	2	0	3	0	1	4
25	13	1	3	3	1	0	2	0	0	0	0	2	1	0	1
26	23	6	3	5			1	3	2	1	1	4	1	3	2
27	31	3	5	1			4	2	1	0	2	5	0	4	3
28	13	3	5	3	2	0	1	1	1	1	0	2	1	0	2
29	6	0	3	2			0	1	0	0	0	1	0	0	1
30	9	1	2	1	3	0	2	2	1	0	1	4	0	2	3
31	12	1	3	0			1	1	0	0	0	2	0	1	1
32	10	0	7	2	1	0	4	0	0	0	0	4	2	0	2
33	6	0	10	0			0	3	0	0	0	3	0	2	1
34	8	1	3	2			1	3	1	1	0	4	0	2	3
35	23	4	5	0	3	0	3	3	0	0	0	6	1	0	5
36	29	11	4	2	1	0	6	2	0	0	0	8	5	1	2
37	34	7	6	5	2	0	7	2	4	4	1	8	4	1	8
38	16	4	2	1	1	0	4	2	0	0	0	6	1	1	4
39	15	2	1	1	1	1	2	3	3	1	2	5	1	1	6
40	26	7	1	0			5	1	3	1	3	5	1	3	5
41	12	1	8	4	2	1	1	5	0	1	0	5	0	2	4
42	18	6	2	1	1	0	1	4	1	1	1	4	1	0	5
43	16	5	4	0			3	1	4	1	2	5	3	0	5
44	11	2	2	0	1	0	5	1	1	0	1	6	4	2	1
45	25	0	5	5	3	0	4	1	1	1	0	5	2	1	3
46	43	7	18	2	2	2	3	3	2	1	2	5	2	0	6
47	13	2	13	3	1	1	2	2	2	1	0	5	3	1	2
48	16	2	6	2	0	1	1	5	1	1	0	6	0	3	4

TABLE VI *S wave data (azimuth in which the first S motion takes place)*

	1	2	3	4	5	6	7	8	9	10	11	12	13	14	15	16	17	18	19	20	21	22	23	24	25	26	27	28	29	30	31	32	33	34	35	36	37	38	39	40	41	42	43	44	45	46	47	48	
Melbourne																																																	Melbourne
Riverview	N **22**° E	N **53**° E	N *41*° E		N 56° E	N 124° E	N **157**° E	N 270° E	N *335*° E	N 186° E	N **90**° E	N **19**° E	N **112**° E	N **125**° E	N **229**° E	N **326**° E	N *0*° E	N **63**° E	N *180*° E	N 148° E	N 216° E	N **74**° E	N 135° E	N 180° E	N 339° E	N *180*° E	N **0**° E	N *220*° E	N 124° E		N 339° E	N **141**° E	N 180° E	N **180**° E	N 206° E	N 138° E	N **318**° E	N 216° E	N *347*° E	N 347° E	N 299° E	N **138**° E	N *118*° E **32**	N **54**° E **22**	N 116° E **286**	N **246**° E **253**	N **252**° E *288*	N 153° E	Riverview
Amboina						70																																											Amboina
Bandung																								*346*				211			**297**	51	220	**116**	**320**													Bandung
Bombay	333	**180**	**76**	N 45° E				**50**			39	**186**										*309*	**315**			*303*	324										27										160	48	Bombay
Djakarta					**201**		**108**			*64*		*135*	295	315	230						**241**			*22*			**26**				**307**	22	*65*	291				*218*	334	**148**	**171**	**180**				173		Djakarta
Hongkong																																							*240*	321	**129**	*333*	*121*				*130*		Hongkong
Hyderabad	306	0	*0*	145				**56**	**270**		**180**	37								*180*		**0**				26	322													**270**							Hyderabad
Irkutsk		**161**										**321**								**302**			**10**			321	**249**										*200*										Irkutsk
Kobe					*90*	**158**	49			**228**				**325**	*270*			**0**	*348*										N 79 E°							**350**	*42*											Kobe
Lembang																																								*225*	301	**104**	*121*			*243*				Lembang
Medan					44																																									**34**	53	Medan
Sapporo					**225**	**141**	*26*										**90**													135	**56**	**270**		154		**27**	**315**											Sapporo
Stalinabad																																					*217*										*270*	Stalinabad
Tashkent	**208**	55						**61**				**204**								**254**							**204**										*160*											Tashkent
Tokyo		**206**																																													Tokyo
Helwan									**214**																																							Helwan
Hermanus																																				*108*												Hermanus
Tamanrasset																																										270						Tamanrasset
Tananarive						*80*						**26**									63	90	180				*180*															*191*				Tananarive
Aberdeen						**292**	**47**																						*153*						296		290										Aberdeen
Almeria						**270**																																										Almeria
De Bilt					*66*	**257**	**9**							*235*									*180*	**230**												*34*			**53**								De Bilt
Erevan																																					**248**	323										Erevan
Granada																																				**90**											Granada
Kew											**54**																																				Kew
Kiruna																														**116**				**143**	**217**	*277*			**73**			*180*		*244*		218	Kiruna
Kirovabad																																					**213**											Kirovabad
København		228	121	274		**248**		*135*			180		*306*		**180**				**63**	**270**	*41*	**0**				**43**	**220**									**119**			**58**				**143**			**33**	København
Makhachkala																																						24										Makhachkala
Moscow		**32**										**232**							255		**138**		**289**												**272**			**88**	23	*36*		327	**197**	26		259	Moscow
Praha					*59*	**262**				281																										**69**										Praha
Tblisi								*331*												97																**210**	344									Tblisi
Toledo																																				241											Toledo
Uppsala	315		**220**		127	*163*	**50**		**221**	256	247				6				264		*249*			102	270	212				77				241	**127**	**255**	**82**		220	**90**		316	**124**	**144**	**147**	25			Uppsala
Yalta																							**324**													34	124	**217**											Yalta
Scoresby sund							*155*			*117*																																					Scoresby sund

Remarks:

Bold type figures are consistent.

Normal type figures are consistent with an S motion half a period later than the first onset.

Figures in italics are inconsistent.

TABLE VIIa *Numbers of consistent and inconsistent data for some Sumatra earthquakes* (Veldkamp 1959)

Nr.	P and PKP		S			S for alternative solution		
	c	i	c	c±180°	i	c	c±180°	i
V 3	17	2	3	1	2	2	0	4
V 5	11	2	2	1	1	0	1	3
V 6	26	3	4	1	1	1	0	5
V 7	23	3	5	2	0	0	0	7
V 8	23	2	4	1	2	1	0	6
V 9	13	0	2	2	1	1	0	4
V 10	13	0	1	3	1	1	0	4
V 11	12	2	2	1	1	0	1	3
V 12	23	1	4	0	2	1	1	4
V 13	15	0	4	0	0	0	1	3
V 16	15	2	3	0	1	0	0	4
V 17	11	0	2	1	0	0	0	3
V 19	22	1	5	4	0	1	2	6
V 20	21	1	2	0	1	0	0	3
V 21	17	0	3	1	1	1	1	3
V 22	15	0	1	0	2	1	0	2

TABLE VIII *The solutions obtained*

No.	Direction of Fault Movement A-axis		Normal to Fault Plane C-axis		Direction of B-axis		Type	Remarks
1	N 280° E,	6°	N 10° E,	3°	N 125° E,	83°	L (P)	Poor evidence; great possible variation in solution.
2	211	6	119	18	318	71	LT	
3	141	10	50	4	300	79	RP	S-data contradictory.
	50	4	141	10	300	79	LP	Alternative solution.
4	158	4	68	5	287	84	LT	
5	50	16	315	18	180	66	RP	S+data contradictory.
	315	18	50	16	180	66	LP	Alternative solution.
6	146	5	326	85	56	0	P	Great possible variation in C- and B-axis.
7	350	2	81	20	255	70	LP	
8	180	40	0	50	90	0	T	Great possible variation in C- and B-axis.

TABLE VIII (continued) *The solutions obtained*

No.	Direction of Fault Movement A-axis		Normal to Fault Plane C-axis		Direction of B-axis		Type	Remarks
9	N 186° E, 25°		N 315 °E, 54°		N 84° E, 24°		PL	Poor evidence.
10	128	15	35	11	271	71	LT	
11	205	26	105	20	342	56	LT	Small change in solution possible.
12	215	20	125	0	35	70	L	Great possible variation in solution.
13	184	11	279	22	70	65	LP	S-data contradictory.
	279	22	184	11	70	65	RP	Alternative solution.
14	25	30	127	20	246	53	LP	Poor evidence.
15	35	5	215	85	125	0	T	Great possible variation in C- and B-axis.
16	160	26	56	26	288	52	RP	S-data poor.
	56	26	160	26	288	52	LP	Alternative solution.
17	247	15	340	10	102	72	RT	Small number of data.
	340	10	247	15	102	72	LT	Alternative solution.
18	199	20	104	14	342	65	LT	Small number of data.
	213	36	115	12	10	52	LT	Another possible solution.
19	165	12	256	5	9	77	RT	
20	145	30	246	20	5	53	LP	
21	100	10	10	0	280	80	L	
22	45	20	225	70	135	0	P	Great possible variation of solution.
23	129	45	34	4	300	45	PR	
24	150	26	242	4	341	64	LP	
25	308	34	208	15	98	52	LT	
26	201	14	105	23	320	63	LT	
27	234	30	135	15	22	56	LT	
28	122	4	30	22	222	68	RP	S-data poor.
	30	22	122	4	222	68	LP	Alternative solution.

TABLE VIII (concluded) *The solutions obtained*

No.	Direction of Fault Movement A-axis		Normal to Fault Plane C-axis		Direction of B-axis		Type	Remarks
29	N 329° E,	30°	N 238° E,	1°	N 147° E,	60°	RP	Poor evidence.
	144	35	235	2	328	55	LP	Another possible solution.
30	113	4	204	8	356	81	LP	
31	335	10	243	10	108	76	RP	Small change in solution possible.
32	245	12	150	23	1	64	LT	Small change in solution possible.
33	158	5	68	3	306	84	LT	
34	159	16	250	2	348	74	RT	
35	116	2	26	0	296	88	L	
36	182	16	87	17	312	66	RP	
37	116	14	207	2	304	76	LP	
38	210	16	115	18	339	66	LT	
39	40	24	145	30	278	50	RT	
40	150	60	295	25	32	15	TR	
41	220	20	130	0	40	70	L	Small variation of solution possible.
	230	30	323	5	61	59	LP	Another possible solution.
42	295	36	38	17	148	49	LP	
	165	12	256	6	14	77	RT	Another possible solution.
43	253	2	163	6	358	84	LT	Conflicting S-data.
	163	6	253	2	358	84	RT	Alternative solution.
44	68	0	158	3	338	87	L	
45	24	28	128	24	252	52	RT	
46	48	36	182	43	298	25	TR	
47	43	30	161	40	288	36	TR	
48	143	7	53	0	323	83	L	

TABLE VIIIa *Some solutions of Sumatra earthquakes* (Veldkamp 1959)

No.	Date	Direction fault mov. A-axis		Normal to fault plane C-axis		B-axis		Type	Remarks
V 3	1933, June 24, $21^h\ 54^m\ 38^s$ 5S 104¼E, s (7.5)	N 71° E, 40°		N 181° E, 20°		N 290° E, 42°		PL	
V 5	1935, Nov. 25, $10^h\ 03^m\ 02^s$, 5½N 94E, s (6.5)	264	54	135	25	33	25	TL	poor
V 6	1935, Dec. 28, $02^h\ 35^m\ 22^s$, ¼S 98E, s (7.9)	18	8	112	26	272	63	LP	
V 7	1936, Aug, 23, $21^h\ 12^m\ 13^s$, 6N 95E, 40 km (7.3)	26	25	133	31	265	48	LP	
V 8	1938, Nov. 15, $21^h\ 00^m\ 16^s$, 5S 99E, s (6.5)	100	34	0	14	251	52	RP	
V 9	1943, June 8, $20^h\ 42^m\ 46^s$, 1S 101E, 50 km (7.4)	214	11	90	71	307	15	PL	poor, great variation possible
V 10	1943, June 9, $03^h\ 06^m\ 22^s$, 1S 101E, 50 km (7.6)	214	11	90	71	307	15	PL	poor, great variation possible
V 11	1946, Mar. 26, $17^h\ 09^m\ 03^s$, 3S 102E, s (6.7)	201	16	108	10	347	71	RP	
V 12	1946, May 8, $05^h\ 20^m\ 22^s$, ½S 99½E, s (7.1)	26	7	292	30	128	59	RP	
V 13	1949, May 9, $13^h\ 36^m\ 18^s$, 5N 95E, s (6.7)	125	57	21	9	286	32	PR	
V 16	1937, July 1, $11^h\ 49^m\ 49^s$, 3N 96E, 110 km (6.7)	45	56	190	30	290	16	PL	
V 17	1937, Aug. 4, $23^h\ 35^m\ 22^s$, 6N 94½E, 120 km (6.0)	68	7	161	20	320	69	RT	
V 19	1938, Aug. 18, $09^h\ 30^m\ 04^s$, 4S 103E, 100 km (6.9)	90	30	320	48	197	26	PR	great variation possible
V 20	1938, Aug. 25, $01^h\ 28^m\ 07^s$, 5S 102E, 70 km (6.9)	10	12	276	18	132	68	LT	
V 21	1943, Nov. 26, $21^h\ 25^m\ 22^s$, 2½S 100E, 130 km (7.1)	14	22	125	42	264	40	PL	
V 22	1944, Jan. 5, $21^h\ 12^m\ 43^s$, 3½S 102E, 60 km (7.0)	24	25	123	19	247	58	LP	

ANALYSIS OF THE DATA

1. 1934, April 10, 7°S 116°E, shallow (fig. 5).

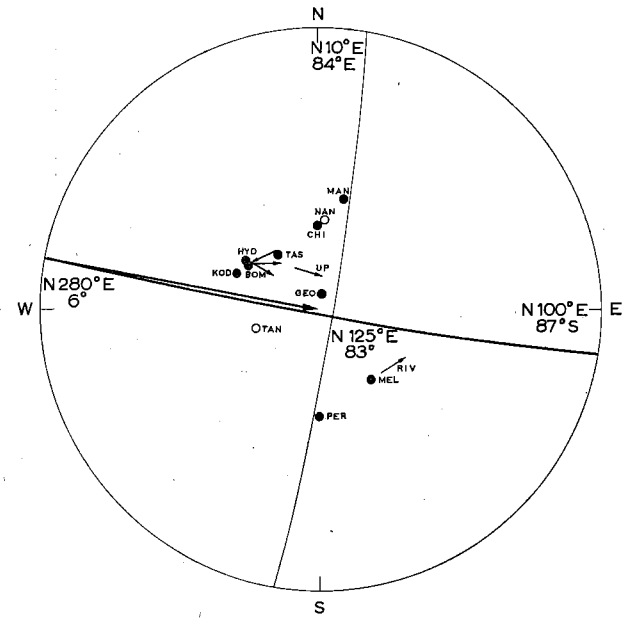

Fig. 5. 1934, April 10, 10h 23m 02s, 7°S 116°E, shallow, M = 6¾.

The number of data is small, and a wide variation in the given position of fault movement, fault plane and B-axis is possible.

Although no serious inconsistencies occur (Nangking D derived from ISS) the solution given is tentative.

2. 1937, September 27, 8°¾ S 110°¾ E, 0.005 R.

The inconsistent C of Tashkent is rather serious, the few others are not being from stations the projection of which is situated near one of the nodal lines. The S data are very homogeneous, unanimously pointing to the given direction of fault movement. Evidence for the solution is fair.

3. 1938, February 1, 5°S 131°½ E, shallow.

There are no serious inconsistencies in P and PKP data, the evidence for the position of the two nodal planes is good. S data, however, are not uniform. The solution gives the best score of S data, the alternative position of fault movement direction and of fault plane, however, cannot be ruled out as a possible solution.

4. 1940, March 21, 10°½ S 107°½ E, shallow.

Evidence of the longitudinal wave data is good, although the number of data is not impressive. The few S data are rather poor, but the direction of the fault movement seems to be fairly well determined.

5. 1940, March 28, 14°¼ N 120°½ E, 0.02 R.

The position of the two nodal planes for longitudinal waves in the focus is fairly well established, the inconsistencies of ZiKaWei and Fordham are both from ISS. The S date are not homogeneous, the choice of the direction of fault movement and of the fault plane is not definite. The difference in consistent data for the solution given is very small as compared with the alternative solution.

6. 1941, June 26, 12°½ N 92°½ E, 0.005 R.

The direction of the fault movement is determined with only a small margin of possible variation. There are no serious inconsistencies, those of Riverview and Scoresby Sund are on all sides surrounded by data of the opposite kind. S data are uniform. The position of the fault plane cannot be established with the data at hand. The dip direction of the fault plane is variable between N 60°E, 50° via N 146°E, 5° to N 230°E, 40°. This means that the transcurrent part of the fault movement can be either right- or left-handed. The partly reverse character of the fault movement is determined with certainty.

7. 1942, April 8, 13°¼ N 120°½, shallow.

The score of consistent data is not very high, but only the C observation of Perth is rather serious and this one is situated not far from one of the nodal lines. The S data are rather uniform. Evidence for the solution is fair.

8. 1942, July 29, 2°¾ S 127°¾ E, shallow.

The inconsistent Tananarive and St. Louis data are not serious. O—C time interval for Tananarive is + 21 sec and St. Louis is surrounded by many data of the opposite kind. The direction of fault movement is determined in such a way as best to be in accordance with the S data. A wide variation in the position of the fault plane is possible, the dip direction of the fault plane is variable between N 134° E, 50° and N 220°E, 40° via N 180°E, 40°. As a matter of fact also the direction of the fault movement is variable to some degree. That the direction of the fault movement is in a southerly direction, however, is certain, and also that the mechanism is of the normal fault type (T). The transcurrent part of the fault movement cannot be determined with the available data. This is an example in which the solution could not be reached with the P and PKP data alone, but only after taking into account also the S wave data.

9. 1943, April 1, 6° ½ S 106°E, shallow (fig. 6).

Evidence for the solution is poor because of the small number of data.

The position of the fault movement is rather well established by the C data of Hyderabad, Tashkent and Djakarta and the D of Agra. The dip direction of the fault plane is variable between N 116°E, 54° and N 160°E, 27°. The solution is classified as tentative.

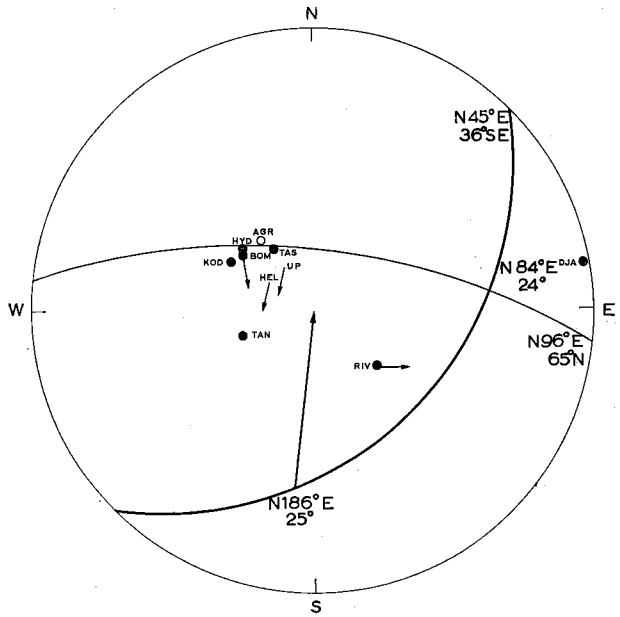

Fig. 6. 1943, April 1, 14h 18m 12s, 6½°S 106°E, shallow, M = 7.0.

10. 1943, May 25, 7°½ N 127°½ E, shallow.

The C′ of La Paz is the only serious inconsistent observation in the longitudinal wave data. The inconsistent S wave of Djakarta is not serious because of the small epicentral distance of about 25°. Evidence for the solution is fair.

11. 1943, November 6, 5°¾ S 134°E, shallow.

No serious inconsistencies, the O—C interval for Florence C′ is —8 sec. The S data are remarkably uniform. Some variation in the given positions is possible because of the small number of data. The evidence for the solution given is fair.

12. 1944, March 31, 5°½ S, 131°E, 0.005 R.

The inconsistent D of Kodaikanal is not serious, it is reported as doubtful. P D of Perth is read as faint and dubious. This is in accordance with the solution in which one of the nodal lines passes near to this station. S data are remarkably uniform. The inconsistent S wave of Djakarta is possibly caused by the small

epicentral distance of 25°. In the solution a wide variation is possible. The direction of fault movement as given in the Table VIII is for an important part determined by the available S data. It is certain that the fault movement is in the S.W. direction and that the block movement is of the left-handed transcurrent fault type. A small pressure and a small tension component of the fault movement are both possible. Evidence for the solution is fair, notwithstanding the small number of data.

13. 1944, April 26, °¾ S 133°½ E, shallow.

The only rather serious inconsistent P is that of Perth. The position of the two nodal planes, however, is determined without any variation, the evidence of the longitudinal waves is fair. The S data are poor, and the alternative solution also given in the Table, has a nearly equal probability.

14. 1944, April 27, 1°S 133°E, shallow.

Evidence for the solution given is rather poor. The inconsistent dilatations of two New Zealand stations are serious. The S data are uniform, the inconsistent S of De Bilt is not serious, de Bilt being situated at an epicentral distance of 113°. Some variation in the given solution is possible without violating the number of consistent data.

15. 1944, November 15, 4°½N 127°½ E, shallow.

The direction of the fault movement can be determined with a negligible margin of variation in position. There are no serious inconsistencies but there is a great variation in the fault plane position possible, with dip directions of N 309° E, 50° via N 35° E, 5° to N 121° E, 50°. This means that the partially normal character of the fault movement is fixed, but also that it is not possible to decide between right- and left-handed transcurrent motions.

16. 1945, October 16, 0°S 123°¾ E, 0.005 R.

No serious inconsistencies. The only reliable S observation of Riverview is in accordance with the solution given in the Table. The alternative solution is also given because the proof for the first solution is slight.

17. 1946, January 17, 6°¼ S 147°¾ E, 0.01 R.

No inconsistent data in the longitudinal wave observations, but because of the small number of data the evidence is rather poor. The S wave evidence is very dubious, the two data of Riverview ($\triangle = 28°$) and Sapporo ($\triangle = 49°$) are conflicting. In the solution given in the Table the observation of Sapporo is assumed to be consistent because this station is farther away from the dangerous zone where the SH part is not recorded on an equal scale with the SV part. It is also possible, however, that the alternative solution is the actual one.

18. 1947, May 27, 1°¾ S 135°½ E, 0.01 R.

The evidence of the longitudinal waves is fair. The S data are homogeneous, but only two in number. There are two positions of the nodal lines which give exactly the same consistent and inconsistent data. We have chosen the solution with the smallest plunge of the fault movement direction as the most probable one.

19. 1948, January 24, 11° N 122° E, shallow.

Djakarta C and Calcutta D observations are rather serious inconsistencies. S wave evidence is fair, especially if we consider that the inconsistent S of Kobe arrives 10 sec late, and therefore represents a doubtful reading. No change of position of any importance to the solution is possible. Evidence fair.

20. 1948, March 1, 3° S 127° ¼ E, shallow.

All data, P, PKP as well as S are very consistent. Evidence for the solution given is good.

21. 1949, March 27, 3°¼ N 127°¾ E, shallow.

In P and PKP no serious inconsistencies, the C of Berkeley has been reported as being dubious. The S data are rather good, the inconsistent data of Uppsala and Copenhagen probably are of SKS waves which must polarize in the plane of incidence. The S of Djakarta is not certain, although in good accordance with the solution, because of the small epicentral distance of 23°. The evidence for the solution is fair. Only a very slight change in position of the nodal planes is possible.

22. 1949, April 23, 7°½ S 120¾ E, 0.00 R.

This is a revision of the earlier solution given as earthquake no. 34 in Table I of RITSEMA, 1957c. In the meantime some more data have been collected, resulting in the solution that is given here. There is no difference in the position of the nodal planes for the longitudinal waves although some more data are known. The inconsistent D of Berkeley is not serious (from ISS bulletin). The newly known S data point to the alternative solution of that originally given as the most probable. The evidence, however, is still poor. A wide variation in the position of the fault plane is possible, from N 340° E, 40° via N 45° E, 20° to N 108° E, 50°. The reverse fault character is certain, the transcurrent component of the fault movement cannot be determined with these data.

23. 1949, June 24, 6° ¼ S 105°¾ E, 0.005 R.

Evidence for the solution is fair, there are no serious inconsistencies. The S data clearly point to a fault movement in S.E. direction. The direction of fault movement given in Table VIII is variable to somewhat steeper values. The classification of the earthquake as to type remains the same.

24. 1949, December 29, 18°N 121° E, shallow.

No serious inconsistencies in P and PKP. The two inconsistent S readings of Djakarta and Bandung ($\triangle = 28°$) are more than 11 sec late and therefore dubious. In the alternative solution the only consistent data are just these two observations. Evidence for the solution given is fair.

25. 1950, September 19, 2° S 138°½ E, shallow.

The great percentage of inconsistent PKP data, 3 on a total of 6, is rather disturbing. All inconsistent observations are from stations at epicentral distances of about 130° where the beginning of the PKP wave is often not clear. The evidence of S is poor in quantity, but rather convincing in quality, clearly pointing to the solution given. Evidence for the solution is fair.

26. 1950, October 8, 3°¾ S 128°¼ E, shallow.

Riverview C and La Paz C′ are serious inconsistencies. Also the high percentage of inconsistent P data of Japanese stations cannot be explained easily, the group being situated far from a nodal line. S data are rather uniform and in good accordance with the solution given. Therefore the evidence of the solution is fair.

27. 1950, November 2, 6°½ S 129°½ E, shallow (fig. 7).

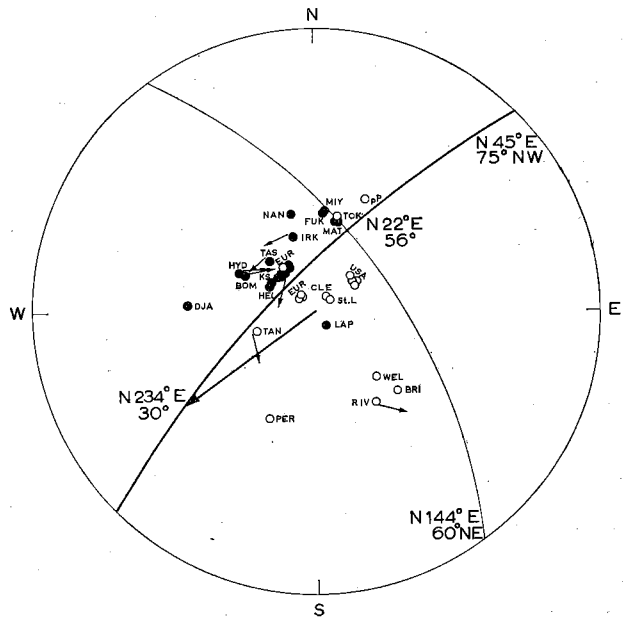

Fig. 7. 1950, November 2, 15h 27m 56s, 7½°S 129°E, 0.03 R, M = 7.5.

P and PKP data very consistent. The only remarkable inconsistency is the C′ of La Paz. S data are also uniform and homogeneous. Evidence for the solution given is classified as good. The possible variation in the solution is negligible.

28. 1950, November 8, 9°½ S 159°½ E, shallow.

For the divergent PKP data (three C′ and five D′) of European stations an explanation is found by the drawing of one of the nodal lines near to this group of data. The inconsistent C of Nangking (ISS) is peculiar, situated in the midst of a dilatation quadrant. S data are poor. That of Riverview is not of the earliest beginning of the wave and, moreover, the epicentral distance of 26° is on the low side for a reliable S reading. The alternative solution cannot be ruled out by the available data.

29. 1951, November 29, °½ N 120°½ E, shallow.

Very meagre data of poor reliability. There are at least two possible solutions giving exactly the same distribution of consistent and inconsistent data. The direction of fault movement is either in N.W. or in S.E. direction. Evidence poor.

30. 1952, May 8, 2°½ N 127° E, shallow.

The inconsistent D observation of Wellington is rather serious, being situated in the midst of a compression quadrant. S data are homogeneous. Evidence is good.

31. 1952, November 6, 5° S 145°½ E, shallow.

The inconsistent D of Quetta is remarkable as it is totally surrounded by consistent data of the opposite kind. S data are few but good. The solution given is a middle position. A variation of some degrees in strike and dip of the two nodal planes not affecting the type of block movement, is possible. Evidence good to fair.

32. 1952, November 28, 6°½ S, 155°½ E, 0.01 R.

No serious inconsistencies in the longitudinal wave date. S data are very uniform and consistent. A variation of some degree in the solution is possible. Evidence is good.

33. 1952, December 24, 5°½ S 152°E, shallow.

No inconsistencies in P and PKP. S data also good. Relatively small number of data, therefore the solution is classified as fair.

34. 1953, April 23, 4°S 154°E, shallow.

The inconsistent C of Djakarta is an emergent onset. Both inconsistent PKP

data are about 10 sec late. S data are uniform and consistent. Evidence for the solution is fair.

35. 1954, July 2, 13°N 124°E, shallow (fig. 8).

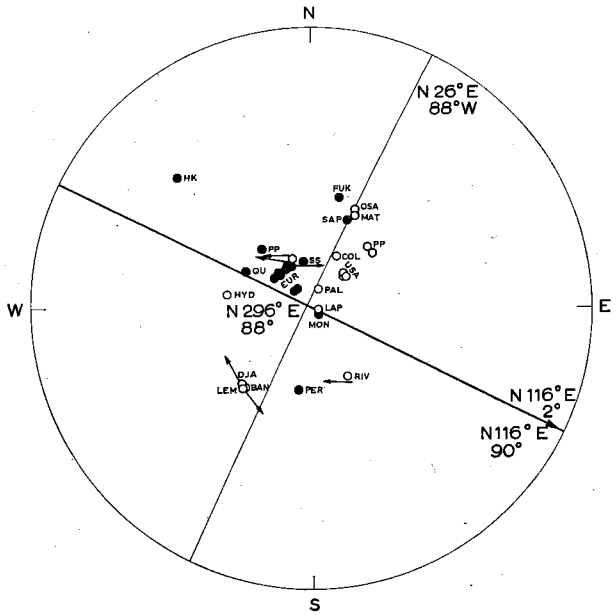

Fig. 8. 1954, July 2, 02h 45m 09s, 13°N 124°E, shallow, M = 7.

The dilatation of Riverview is a serious inconsistency. That of Kiruna is on all sides surrounded by data of the opposite kind. S data are remarkably uniform. Evidence is good.

36. 1955, March 31, 8° N 124° E, 0.005 R.

There are many inconsistent data, caused by one of the nodal lines passing through the regions where the numerous European and N. American stations are situated. Only College C and Riverview D are serious. The S data are rather good, clearly pointing to the solution given.

37. 1955, May 17, 6°½ N 94° E, shallow.

The many inconsistent European D and North American C′ data are caused by the proximity of one of the nodal lines in the diagram. The computed position of the two nodal planes for longitudinal waves is not subject to variations. S data are not very satisfying. A rather high percentage is in conflict with one or both of the two possible solutions. The readings of Kobe,

Hermanus and Toledo are reported to be dubious. Still the evidence for the solution is given as fair. The remaining data clearly point to the solution given.

38. 1955, May 29, 10° S 110°½ E, shallow.

The inconsistent P data of East Europe and Central Asia can be caused by the nodal line passing through these regions. The inconsistent C of Riverview is serious and cannot easily be explained. S data are very homogeneous and invariably pointing to the solution given. Evidence is fair.

39. 1955, September 15, 5° S 134°½ E, shallow.

The inconsistent Kiruna C (dubious), Wellington C (small) and Cleveland C′ (BCIS bulletin) are all surrounded by many more dilatation data. The S data are not very homogeneous. The choice of the solution is based mainly on our own observations of the seismogram copies of Russian stations. The evidence for the solution is fair.

40. 1956, February 12, 19° N 119°½ E, shallow.

All inconsistent data are surrounded by many data of the opposite kind and are therefore not serious. The inconsistent readings of the Indonesian stations were about 20 sec early for the S wave and therefore no great value is attached to these data. The position of the fault plane is determined within a margin of a few degrees. The direction of fault movement has been chosen in such a way that the S wave of Riverview is consistent. If we do not accept this criterion a rather wide variation in the direction is possible. The earthquake type, however, is definitely determined as T, e.g. as a normal fault movement. Evidence fair.

41. 1956, May 22, 4° S 152°½ E, 0.08 R.

The inconsistent Medan D is not serious, being read as dubious and faint. The large percentage of inconsistent PKP data in Europe is possibly caused by the proximity of one of the nodal planes. The two nodal planes are taken so that a maximum of S data is in accordance with the solution. There is some variation in the positions possible. A second solution with exactly the same consistent and inconsistent data is also given. The first solution is preferred because the S wave of Riverview is more in accordance with this solution, and because one of the nodal lines passes nearer to the many inconsistent PKP data of Europe than in the other solution. Evidence is fair.

42. 1957, February 10, 10° N 126° E, shallow.

Of the inconsistent data only the D of Hongkong and the two D′ of N. American stations are serious, the few others being surrounded by many data of the opposite kind. The S data are rather good and clearly point to the solution given. A second solution in which the C of Uvira is inconsistent and

the two PKP of N. America are consistent is also given. The score of the S data is somewhat less in this solution. The reason that, in spite of this, the second solution is also given is the great accordance of it with the solutions of the two aftershocks nos. 43 and 44.

43. 1957, February 10, 10°½ N 126°½ E, shallow.

The Eureka inconsistent C is not serious. A small variation in the position of the fault plane can make the observation consistent. More serious are the inconsistencies of Djakarta, Lembang, Bandung and Hongkong. A possible cause lies in the general unrest following the main shock which occurred only 18 min earlier. The S data too are not uniform. These readings, already difficult under normal conditions, undoubtedly have been influenced by the unrest following the preceding shock. The evidence for the solution given is fair to poor.

44. 1957, February 11, 10° N 126° E, shallow (fig. 9).

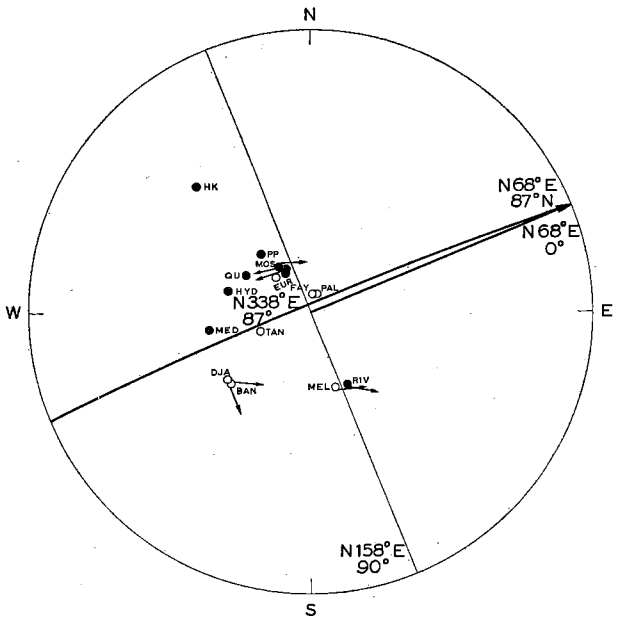

Fig. 9. 1957, February 11, 01h 14m 44s, 10°N 126°E, shallow, M = 6½.

The inconsistent D of Belgrade and Copenhagen of which the times are not reported are not serious. The S data are remarkably uniform. Although the number of data is not great the evidence for the solution is fair. It is remarkable

that the position of the two nodal planes for longitudinal waves and the direction of fault movement in the two aftershocks nos. 43 and 44 is very nearly the same. The main shock, no. 42, shows also a lefthanded transcurrent fault movement but the direction of fault movement differs about 45° from that of the two aftershocks.

45. 1957, March 23, 5°½ S 131° E, 0.01 R.

The high proportion of inconsistent PKP data is rather disturbing. Differences between observed and computed time are rather high, but about equally distributed amongst the consistent and inconsistent PKP data. The group of PKP data is surrounded on nearly all sides by dilatations, this is the reason that we assume the C′ data to be inconsistent. The S data are not bad, the observation of Kobe was reported as dubious. The evidence for the solution given is fair.

46. 1957, April 16, 4°½ S 107°½ E, 0.09 R (fig. 10).

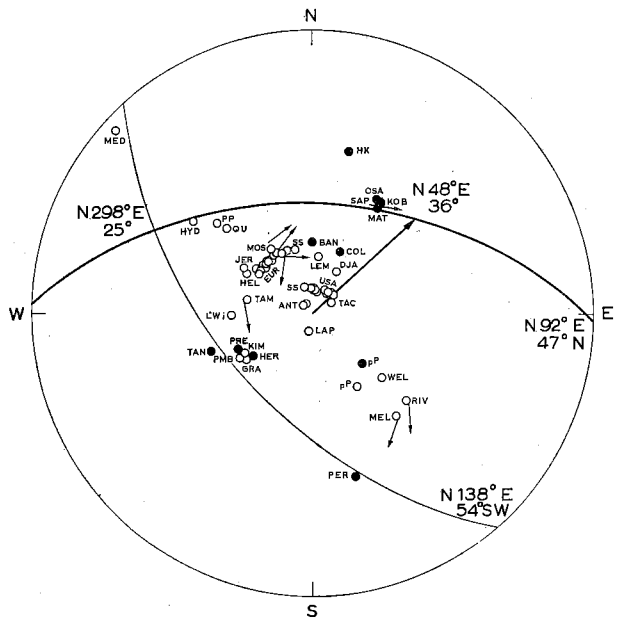

Fig. 10. 1957, April 16, 04h 04m 04s, 4½°S 107½°E, 0.09 R, M = 7½.

Of the inconsistent P and PKP data only College C (from ISS) is rather serious, all the others are surrounded by many data of the opposite kind.

S data are not very homogeneous. Still, the solution given is clearly to be preferred above the alternative solution with the same position of the nodal lines. Evidence fair.

47. 1957, May 2, 7°½ S 120° E, 0.09 R.

No serious inconsistencies, all being surrounded by many data of the opposite kind. S data seem to point to a more northerly direction of the fault movement, but this is contradicted by the P and PKP data. In this case of a deep-focus earthquake the S data of nearby stations as Djakarta and Lembang (△ about 13°) can be used because of the small angle of incidence in the station. The evidence for the solution given is fair.

48. 1957, June 22, 1°½ S 137° E, shallow.

The inconsistent D of Kobe, and of Kiruna, is rather disturbing especially as the two stations are situated in the same azimuth. The S data are rather homogeneous. Evidence fair.

Here follow some remarks on the reliability of the solutions of 16 Sumatra earthquakes that have already been published. The numbers given to the shocks are those of the original publication of VELDKAMP (1957). See also Table VIIa and VIIIa.

V 3. 1933, June 24, 5° S 104° E, shallow.

No serious inconsistent P data. C of Vladivostok is surrounded by data of the opposite kind; and that of Sverdlovsk is situated near to a nodal line. It is not possible to change the position of the fault plane for more than a few degrees. The direction of the fault movement has been chosen in such a way that the best agreement with the S data is reached. Evidence fair.

V 5. 1935, November 25, 5°½ N 94° E, shallow.

Small number of data. The four S data form the base for the determination of the position of the auxiliary nodal plane and thus of the direction of fault movement. Evidence poor.

V 6. 1935, December 28, °½ S 98° E, shallow.

The C of Djakarta is the only serious inconsistency; the others being surrounded by data of the opposite kind (Melbourne), or being situated near to one of the nodal lines (Medan). S data uniform. Evidence fair.

V 7. 1936, August 23, 6° N 95° E, 0.00 R (fig. 11).

No serious inconsistencies. S data very consistent. Possible change in solution negligible. Evidence good.

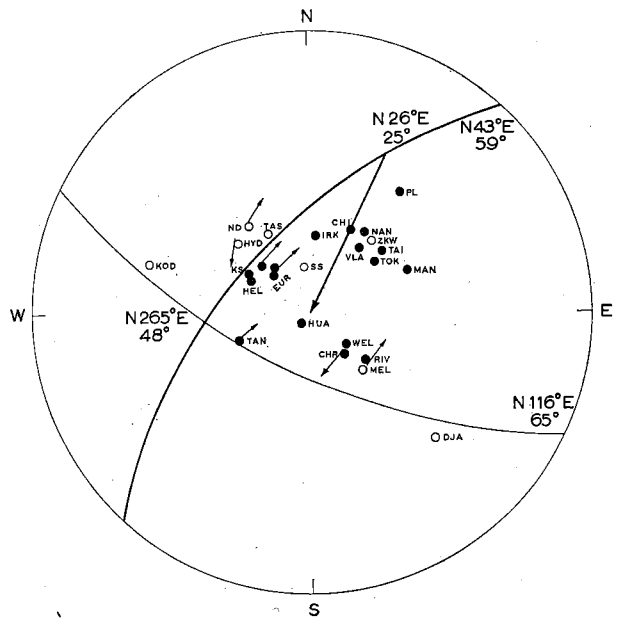

Fig. 11. 1936, August 23, 21h 12m 13s, 6°N 95°E, 0.00 R, M = 7.3.

V 8. 1938, November 15, 5° S 99° E, shallow.

Inconsistent D of Tucson remarkable, being situated in the midst of a compression quadrant. S data not very convincing, de Bilt and Simferopol being inconsistent. Evidence fair.

V 9. 1943, June 8, 1° S 101° E, 0.005 R.

Small number of data. Important variation in the solution given is possible. The reverse character of the fault plane movement is definitely determined. Evidence poor.

V 10. 1943, June 9, 1° S 101° E, 0.005 R.

Aftershock of no. V 9 with exactly the same characteristics. Evidence poor.

V 11. 1946, March 26, 3° S 102° E, shallow.

Small number of data. Sapporo C and Wellington D inconsistent. The few S data are rather good. Evidence fair to poor.

V 12. 1946, May 8, °½ S 99°½ E, shallow.

Inconsistent D of Tucson not serious, surrounded by many compression data. S wave data rather uniform. No change in position of fault plane and direction of fault movement possible. Evidence fair.

V 13. 1949, May 9, 5° N 95° E, shallow.

No inconsistencies. Evidence fair.

V 16. 1937, July 1, 3° N 96° E, 0.01 R.

The inconsistent D of Tucson, and Scoresby Sund, are surrounded by compressions. The position of the fault plane is determined very certainly. The direction of fault movement is variable over more than 10° in the fault plane. The solution given is a mean value of the fault movement. Evidence fair.

V 17. 1937, August 4, 6° N 94°½ E, 0.01 R.

Very small number of data, but very consistent. Evidence fair.

V 19. 1938, August 18, 4° S 103° E, 0.01 R.

Inconsistent D of Hongkong not serious. S data remarkably uniform. Variation in direction of fault movement is small, but in the position of the fault plane it is rather great. The solution gives an average position of the fault plane. (See also RITSEMA 1957c).

V 20. 1938, August 25, 5° S 102° E, 0.01 R.

Inconsistent C of New Delhi of no influence on the solution. Evidence of longitudinal waves is good. S data are poor, only three in number. A change in the solution is not probable. Evidence fair.

V 21. 1943, November 26, 2°½ S 100° E, 0.015 R.

S data not very uniform. Inconsistent De Bilt rather serious. Evidence fair.

V 22. 1944, January 5, 3°½ S 102° E, 0.005 R.

No inconsistencies in small number of P data. S data conflicting. The solution given has been chosen on the analogy of the other Sumatran earthquake mechanisms. The alternative solution, however, is equally probable with the same number of consistent and inconsistent data.

HODGSON (1957) published the solutions of four other earthquakes from the region under consideration here. For two of these the position of the two nodal planes for longitudinal waves in the focus are known, for the other two the positions are indefinite. With the help of the S wave data of Indonesian stations the most likely fault plane for the first two earthquakes could be selected. The solutions follow in Table VIIIb.

DISCUSSION OF RESULTS

All known fault plane solutions of the region are shown on the maps of figures 12, 13 and 14. The results previously reached (RITSEMA 1957c, Veldkamp 1959) are included, also the solutions of two earthquakes recently published by HODGSON (1957).

The solutions are divided according to the depth of the focus; figure 12 gives the solutions of shallow shocks, fig. 13 of intermediate, and fig. 14 of deep shocks.

In total there are 20 Sumatra earthquakes, 41 of Java and the lesser Sunda Islands, 35 of the Philippines, 15 of New Guinea and 11 of the Solomon Islands.

Type of earthquake mechanism

From Table VII, giving the numbers of consistent and inconsistent data for the individual solution of the 48 new earthquakes it is seen that the resulting percentages for longitudinal waves are in close concurrence with the same derived from earlier studies (RITSEMA 1957c): 7 out of 8 P data are consistent, 3 out of 4 PKP data and about 3 out of 4 PP data. From the S data of the individual earthquakes it is seen that it is not always easy to choose between the two possible positions of the fault plane; and even that it is sometimes difficult to state if an individual earthquake is of the "one-couple type" or of the "two-couple type". The overall percentage figures, however, show a clear preference for the fault motion type of Keylis Borok (47 % consistent, 21 % inconsistent, 32 % with a consistent polarization angle but an opposite sense) above the strain release type of Honda (25 % consistent, 54 % inconsistent, 21 % with a consistent polarization angle but an opposite sense).

TABLE VIIIb *Solutions of Hodgson* (1957)

	Direction fault movement	Normal to fault plane	B-axis	Type	Remarks
1955, Aug. 16, $11^h\ 46^m\ 48^s$, 6°S 155°E, 0.03 R (M=7)	N 232° E, 19°	N 139° E, 9°	N 25° E, 69°	RP	fair
1955, Aug. 21, $17^h\ 33^m\ 58^s$, 3°S 137½°E, Shallow (6¾)	244 18 344 30	344 30 244 18	127 54 127 54	LP RP	fair alternative solution
1955, Oct. 13, $09^h\ 26^m\ 45^s$, 9½°S 161°E, Shallow (6¾)		not defined		P	
1956, Jan. 31, $09^h\ 17^m\ 14^s$, 4°S 152°E, 0.06 R (7)		not defined		T	

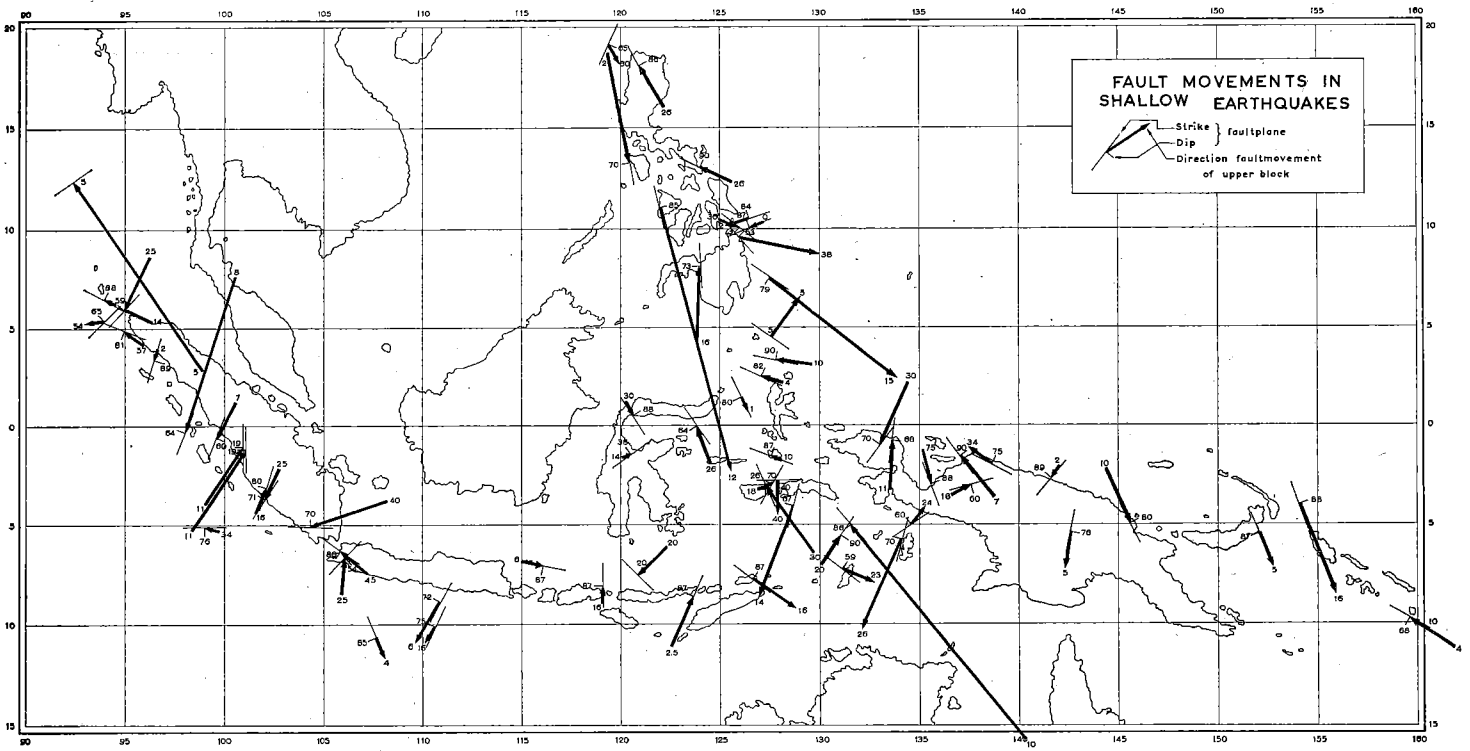

Fig. 12. Solutions for shallow earthquakes (dips indicated in degrees).

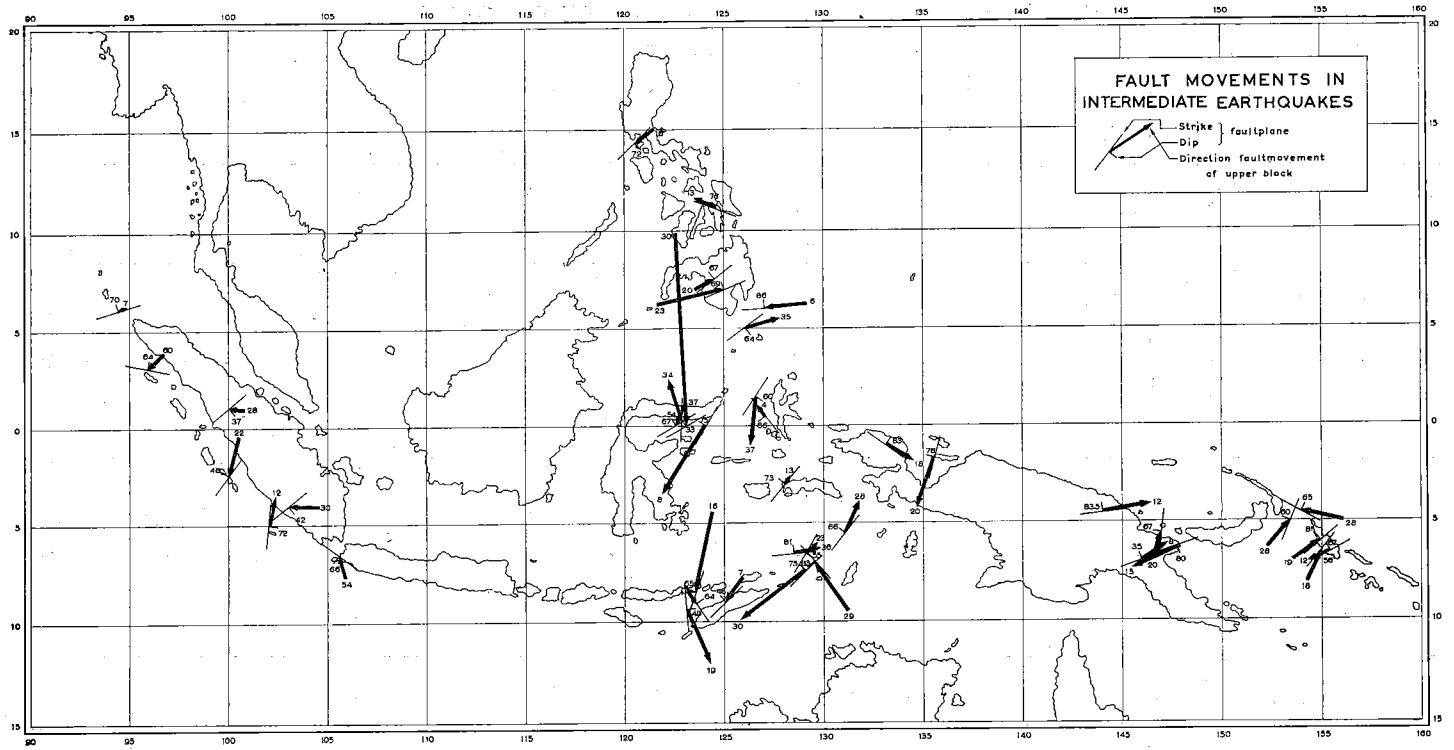

Fig. 13. Solutions for intermediate earthquakes (dips indicated in degrees).

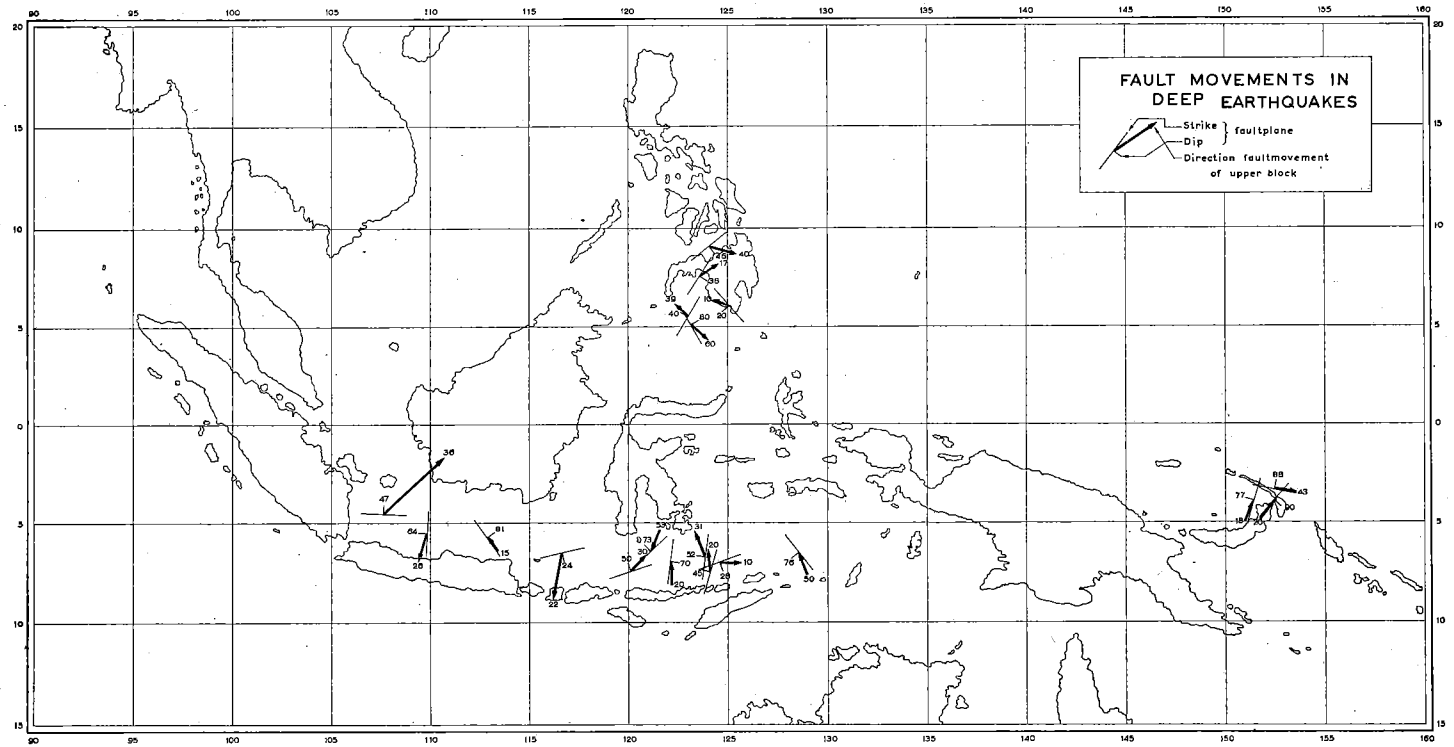

Fig. 14. Solutions for deep earthquakes (dips indicated in degrees).

In order to investigate the distribution of consistent and inconsistent S data in different directions, the S data of the individual earthquakes were reconsidered as if originating from one and the same earthquake focus. The earthquakes of Table VII with less than 4 S data were excluded, also those with an important possible variation in the solution. The selected shocks amount to 34 with an average of 6—7 S data per shock[1]).

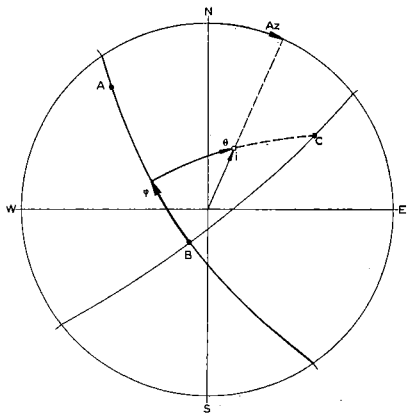

Fig. 15. Co-ordinates of a station with respect to the hypocentre (azimuth: Az and angle of departure: i) and co-ordinates with respect to the fault plane (angle with the B-axis φ, and angle δ measured from the fault plane).

In order to plot all S data in one figure it is necessary to know the angles δ and φ (see figure 15) which determine the position of the various stations with respect to the fault plane. Using Wulff's stereographic net, it is easy to confer the co-ordinates of a point given by azimuth North through East (Az) and angle of departure from the focus (i) into the co-ordinates δ (the angle with the fault plane) and φ (the angle with the B-axis, measured in the fault plane). This has been done with the S data of these 34 shocks.

The newly arranged data were divided into equal δ-groups. Numbers and percentages of the three kinds of S data were calculated for δ-intervals of 10° (Table IX, fig. 16). Data from the compression quadrants were taken together in the + groups, those of the dilatation quadrants in the — groups. The fault plane is given by $\delta = 0°$.

The presence of inconsistent data, with nearly constant percentages of 20—25% is apparently independent of the position of the fault plane, and must therefore be caused by other influences than those of the focal region. Possible reasons are the difficulty of determining the exact commencement of the S wave, and changes of the polarization direction of the S wave by non-horizontal discontinuities encountered by the wave along its path from the focal region to the recording station.

---

[1]) The earthquake nos: 4, 6, 8, 13, 15, 16, 17, 18, 22, 25, 28, 29, 31, 33 were excluded.

TABLE IX

Numbers and percentages of consistent S data, of inconsistent S data and of S data with a consistent polarization direction but an opposite sense for ϑ intervals of 10°

	c	c±180°	i	c	c±180°	i
+ 90°						
	1	0	0	100	0	0
+ 80						
	2	0	0	100	0	0
+ 70						
	0	0	0	—	—	—
+ 60						
	1	1	0	50	50	0
+ 50						
	2	1	1	50	25	25
+ 40						
	2	4	7	15	31	54
+ 30						
	11	8	4	48	35	17
+ 20						
	26	14	8	54	29	17
+ 10						
	16	16	9	39	39	22
0						
	14	10	5	48	35	17
— 10						
	4	9	8	19	43	38
— 20						
	9	3	3	60	20	20
— 30						
	4	4	2	40	40	20
— 40						
	6	0	1	86	0	14
— 50						
	6	2	0	75	25	0
— 60						
	0	0	1	0	0	100
— 70						
	1	0	1	50	0	50
— 80						
	0	0	0	—	—	—
— 90						

At acute angles with the fault plane ($-20° < \delta < +20°$) the percentages of consistent data and of the data with consistent polarization direction but opposite sense, are practically the same. This is just what could be expected because amplitudes in these directions are very small in the "single couple" model and the onsets consequently will be very difficult to read.

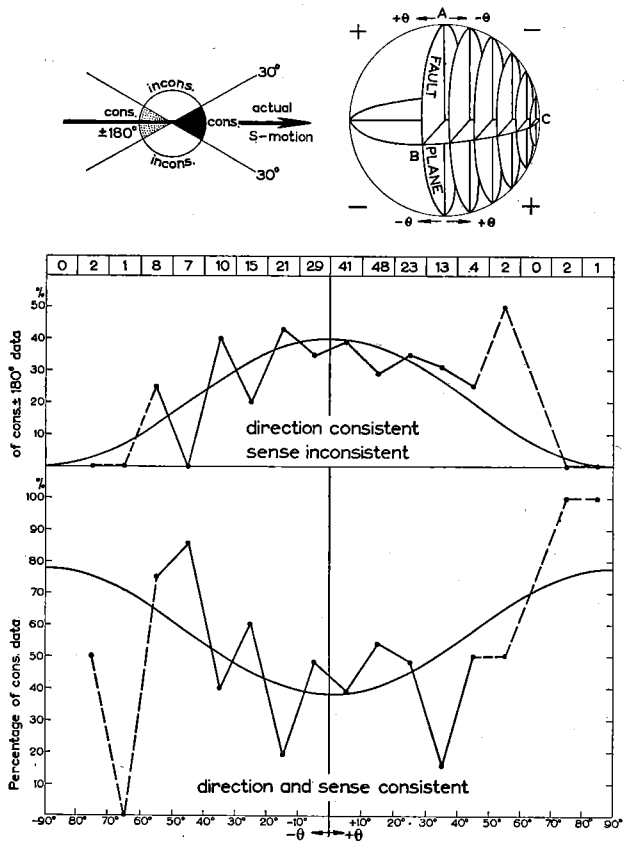

Fig. 16. Percentages of consistent S data and of S data with a consistent polarization direction but with an opposite sense, as a function of the angle with the fault plane δ.

At greater angles with the fault plane the percentage of consistent data increases and that of the data with a consistent direction but inconsistent sense decreases. This also is in accordance with the assumed S wave generation in the focal region because in this model the amplitude of S increases in proportion to $\sin^2 \delta$ and consequently the onsets can be read with more certainty.

For small angles of δ the S-onsets are read accurately in about 1 out of 3 cases, in directions about perpendicular to the fault plane in 4 out of 5 cases.

It may be concluded than that it seems very unlikely that the generation of S waves in the earthquake foci differs appreciably from the assumed "single couple" theory.

Earthquake types

The distribution of earthquake types is shown in figure 17. It is clear that in all regions transcurrent faults prevail. This seems to be more pronounced in the New Guinea and Solomon Islands region. In the Sunda and the Philippines arcs there is a tendency for higher percentages of normal fault movements at great depths. Percentages of dextral (R) and sinistral (L) transcurrent fault movements are about the same at different levels. The overall picture is that of a predominance of transcurrent faults of more than 4 times the value that would be reached with a random orientation of the fault plane and fault movement (see RITSEMA 1957c). That the percentage of transcurrent fault movements in the "Pacific" regions of New Guinea and the Solomon Islands is still higher is possibly influenced by the smaller number of data for this region.

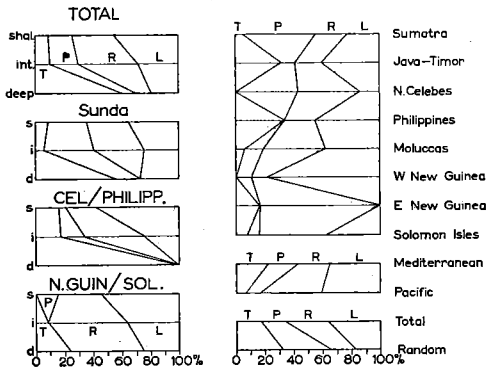

Fig. 17. Geographical distribution of earthquake types
P — mainly reverse.
T — mainly normal.
R — mainly dextral.
L — mainly sinistral.

In this connection it is suggestive that HODGSON (1957) gives two additional solutions for this region in which the earthquake type definitely could be established as normal and reverse respectively, and not as transcurrent (Table VIIIb).

Percentages of combined normal and reverse fault earthquakes are about 25% higher in the "Mediterranean" zones of Sumatra, Sunda arc, Celebes, and Philippines, than in the "Pacific" zones of the Solomon Islands and New Guinea. The same tendency has already been shown to exist in other parts of these major earthquake zones (RITSEMA 1957a).

If we consider the type distribution on a smaller scale, i.e. in smaller detail regions, some clear differences show.

In the Sumatra region including the Strait Sunda, normal or partly normal fault motions are nearly absent (12P, 1T, 5R, 5L).

In the region of Java-Timor reverse fault motions are nearly absent (7T, 2P, 4R, 9L.

In the Banda Sea and Moluccas transcurrent fault motions are the most dominant (1 T, 2 P, 6 L, 7 R).

In N. Celebes it is the absence of normal fault motions that is most conspicuous (3 P, 0 T, 3 R, 1 L).

In the Philippines the absence of reverse fault motions and the high percentage of left handed-sinistral-transcurrent fault motions are very striking (10 T, 0 P, 13 L, 6 R).

In New Guinea and the Solomon Islands region the near absence of any normal and reverse fault motions is the most conspicuous. In West N. Guinea sinistral fault motions are predominant, (7 L, 1 R, 1 P, 0 T), in East N. Guinea dextral (5 R, 0 L, 1 T, 0 P), and in the Solomon Islands region percentages are equal (6 R, 5 L, 1 P, 1 T).

Magnitude of the shocks

In Table X earthquake types are arranged against the magnitude of the shocks. It is clear that there is no relation between the two. In any selected magnitude range the percentage of transcurrent, normal and reverse type shocks is about the same.

TABLE X *Earthquake types against magnitude*

Magnitude	T	P	R	L
$\geq 7\frac{1}{2}$	2	3	3	9
7—7.4	8	8	17	15
$6\frac{3}{4}$—6.9	8	5	7	13
$<6\frac{3}{4}$	3	5	10	8

From the maps of figures 12—14 it is seen, however, that there is a tendency for the fault movements of the larger earthquakes to be orientated in N.—N.W. to S.—S.E. directions. This is true for all seismic zones in the region.

The fault movements of the smaller earthquakes, on the other hand, show a tendency to be orientated in directions about perpendicular to the local, structural lines.

As a matter of fact, this is not a rigid rule to which all earthquakes conform, there being too many clear exceptions. Moreover, we must bear in mind that

the uncertaities in the solutions of these large shocks in general are more important than in the somewhat smaller shocks. Often it seems to be difficult to determine the mechanism of just these large earthquakes. But, as the possible implications of such a dependence of the orientation of the fault movements on the magnitude of the shocks in the region may be of importance, the tendency is stressed here.

Plunge of the fault motions, dip of the fault planes, and plunge of the B-axes

Mean values of the plunge of the fault motions, the dip of the fault planes, and the plunge of the B-axes were calculated for shallow, intermediate and deep earthquakes (Table XI).

TABLE XI *Average values*

	Plunge fault motion	Dip fault plane	Plunge B-axis
Shallow	19°	69°	57°
intermediate	22	65	53
deep	29	57	38
total	21	66	53

The single values are rather erratic, but the mean values do show clear tendencies that confirm the earlier conclusions that were reached for about half of the material used now (RITSEMA 1957c).

On the average the fault motion is steeper the deeper the earthquake has its focus, but in only 8% of the total material was the plunge of the motion larger than 45°.

Fault planes mostly dip steeply. The fault planes of the deeper shocks on the average dip at a smaller angle than those of shallow earthquakes. There are 19 earthquakes (15%) with a fault plane dipping at a lesser angle than 45°. More than half of these solutions, however, are classified as poor or are variable in a wide range. That means that the average dip of the fault plane most probably is larger than indicated by the figures of Table XI.

B-axes mostly plunge steeply. This is especially true for shallow, and in a lesser degree also for intermediate shocks. Most of the B-axes of deep earthquakes plunge at a lesser angle than 45°. In only 25% of the deep shocks the B-axis plunges more steeply than 45°, whereas in only 25% of the shallow shocks the B-axis plunges at a lesser angle than 45°. Moreover, the percentages of poor solutions amongst these last groups is larger than in the main groups, which only accentuates the difference between shallow and deep shocks.

Patterns of B-axes

For each geographical group of earthquakes i.e. Sumatra, Java and Lesser Sunda Islands, N. Celebes and Philippines, and New Guinea and Solomon Islands, the B-axes have been brought together in a single stereographic diagram of Wulff. The individual data were plotted with respect to the direction of the structural lines in the region of the epicentre. Fig. 18 gives the directions of the structures that have been adapted to this purpose. Figures 19—22 show the diagrams for the four geographical groups. B-axes indicated by black dots are from reliable solutions, open circles indicate B-axes of poor solutions or solutions with a wide possible variation.

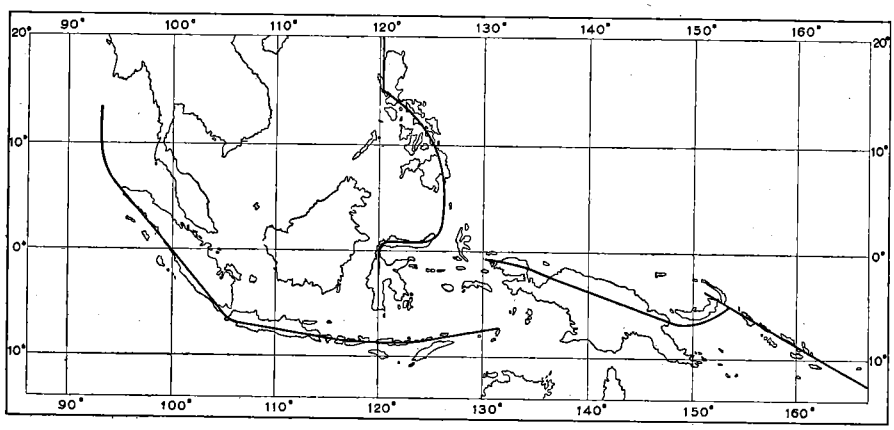

18. The direction of the structural lines in the region of S.E. Asia.

The diameter of the circles differ for shallow (great), intermediate and deep (small) earthquakes. The two half-arrows represent the motion directions of the two adjacent blocks with respect to each other. The length of the arrows is proportional to $E^{\frac{1}{4}}$, where $\log E = 11.4 + 1.5\,M$. The horizontal line PP in the diagram is always the direction parallel to the structural lines in the region discussed. The upward line in the diagrams which is perpendicular to the arc, is directed towards the Asian continent for figures 19—21 and towards the Pacific Ocean for figure 22.

Most of the B-axes in the Sumatra region (figure 19) are concentrated between two planes with a common strike making an angle of about 30° with that of the arc and dipping under angles of + 70° and — 70° respectively. It is remarkable how clearly the fault motions are directed either perpendicularly or parallel to the strike direction of these two planes. No dependency of the direction of fault motion on magnitude is evident.

The concentration of B-axes at the right-hand side as seen from the Asian continent direction is striking.

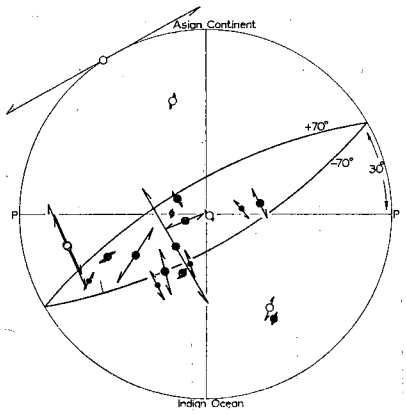

Fig. 19. Stereographic projection of the directions of B-axes of Sumatran earthquakes with respect to the direction of the geological structures (indicated by the line P—P).

full circles:	reliable solutions.
open circles:	poor solutions with a wide possible variation.
great diameter:	shallow earthquakes.
intermediate diameter:	intermediate earthquakes.
small diameter:	deep earthquakes.
half arrows:	motion directions of the two adjacent fault blocks.

Most of the B-axes in the Java—Lesser Sunda Islands region (fig. 20) are concentrated between two planes striking in the direction of the structural lines and dipping 50° and 90° under the Asian continent side. Here also the fault motions show a clear tendency to be directed either perpendicularly or parallel to the structural line. Most B-axes are concentrated at the right-hand side as seen from the Asian continent.

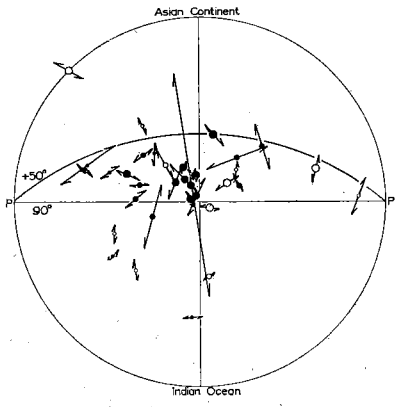

Fig. 20. Stereographic projection of the directions of B-axes of Java and Lesser Sunda Islands earthquakes with respect to the direction of the geological structures.

Figure 21, showing the B-axes of the N. Celebes—Philippines arc, is the least striking. Most B-axes are concentrated between two planes striking in the direction of the structural lines and dipping + 70° and — 70°. The direction of fault motion is rather erratic, especially that of the larger earthquakes. The

small magnitude shocks show a tendency to fault motions perpendicular to the structural lines. Most B-axes are concentrated at the left-hand side as seen from the Asian continent. The direction of the structures in this area changes from W—E in N. Celebes to S—N in Mindanao to about SE—NW in the S of Luzon and back again to S—N in Luzon. It is not surprising therefore that the least system can be found in the directions of the B-axes of the earthquakes of this region.

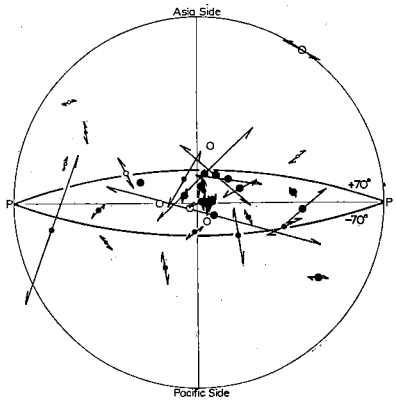

Fig. 21. Stereographic projection of the directions of B-axes of earthquakes of N. Celebes and the Philippines with respect to the directions of geological structures.

In the diagram of the New Guinea—Solomon Islands earthquakes the B-axes are concentrated between two planes striking in a direction that makes an angle of about + 30° with that of the structural lines and dipping + 60° and — 80° under the Pacific Ocean side (fig. 22). Directions of fault motion are again clearly concentrated perpendicularly or parallel to the strike direction just mentioned. There is a tendency of the larger earthquakes to fault motions parallel, and of the smaller shocks for fault movements perpendicular to the zone.

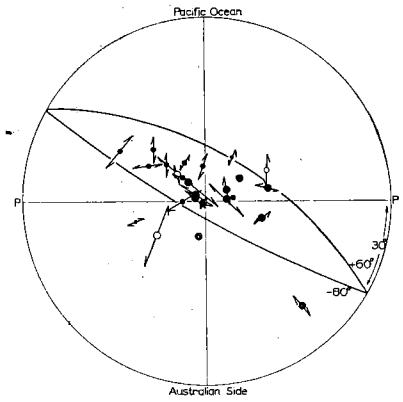

Fig. 22. Stereographic projection of the directions of B-axes of earthquakes of New Guinea and the Solomon Islands with respect to the direction of geological structures.

Directions of principal stresses

If we assume that the "fling" (BYERLY and STAUDER, 1958) along the fault plane, i.e. the actual motion of the two fault blocks relative to each other, causes the pattern of initial motion of longitudinal and transverse waves around the focus, and not the release of stresses as assumed by HONDA c.s. (1957), we may further ascribe these motions to a system of principal stresses.

The angle α between the directions of the greatest stress and the fault motion depends on the value of the angle of internal friction β according to

$$\alpha = 45° - \tfrac{1}{2}\beta$$

For a mean value of β of 40° the angle α is about 25°. It is possible then to determine, in each individual case from the position of the fault plane and the direction and sense of the fault motion, the direction of the principal stresses that in the case of a homogeneous fault rock could have caused the earthquake. These directions combined in one diagram for each geographical group seem to be arranged in certain patterns (fig. 23—26). These patterns are most regular if

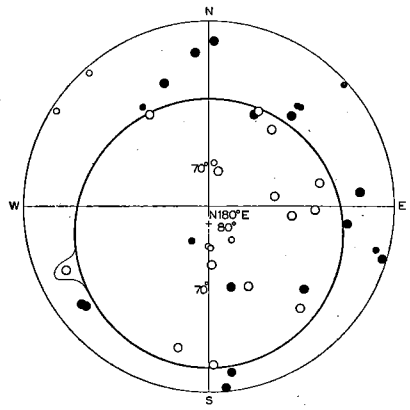

Fig. 23. Stereographic projection of the directions of principal stress components of Sumatran earthquakes.

Full circle: largest compressive stress.
Open circle: smallest compressive stress.
Great diameter: reliable solutions.
Small diameter: poor solutions or with a wide possible variation in parameters.

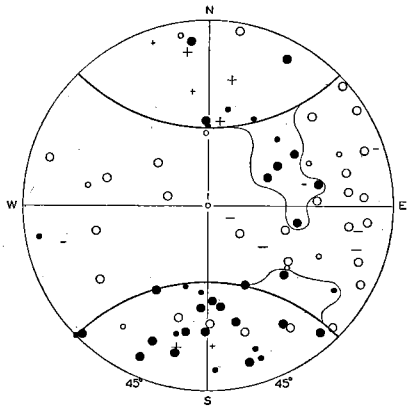

Fig. 24. Stereographic projection of the directions of principal stress components of Java and Lesser Sunda Islands earthquakes (+ and — signs indicate the largest and smallest compressive stresses respectively of earthquakes of N. Celebes. Large marks pertain to reliable solutions, small marks to poor solutions).

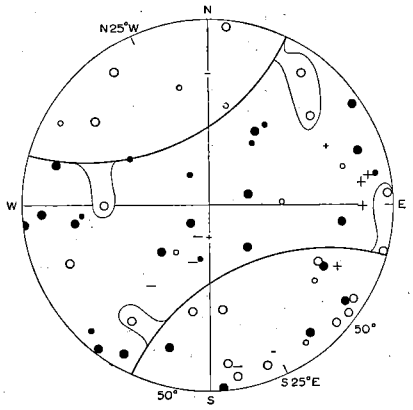

Fig. 25. Stereographic projection of the directions of principal stress components of earthquakes in the Philippines (+ and — signs indicate the largest and smallest compressive stresses respectively of earthquakes in the Moluccas Islands region. Large marks pertain to reliable solutions, small marks to poor solutions).

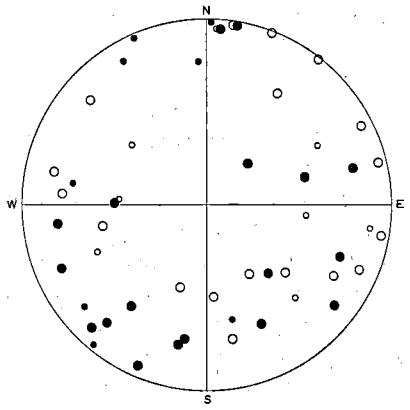

Fig. 26. Stereographic projection of the directions of principal stress components of earthquakes of New Guinea and the Solomon Islands.

the angle between the directions of fault motion and principal compressive stress is supposed to be 20° to 30°. The largest compressive stress is indicated as a black circle, the largest tensile stress (actually the smallest compressive stress) by an open circle. Small circles are poor solutions or solutions with a wide possible variation of parameters.

Figure 23 shows the directions of the principal stress components determined for $\alpha = 30°$ of the earthquakes of the Sumatra region. It will be seen that nearly all "tensions" are confined to a cone with top angle of 70° around the direction N 180° E, 80°, and that all "pressure" components are arranged around this cone with a preference for about N.E.—S.W. directions. This could mean that the Sumatra region is subject to a horizontal tangential pressure with a minimum of pressure in the vertical (radial) direction. These stresses are released by reverse faulting mostly in a direction that is about perpendicular to the zone, but also in other directions (VELDKAMP, 1959).

The data on the Java and Lesser Sunda Islands are brought together in figure 24. Excluded are the data of C. and N. Moluccas where the structural lines change direction. Here an angle α of 20° has been used. It is seen that the vast majority of the "pressure" components is directed in the solid angle of 45° around the direction N 0° E, and most of the "tension" components outside this double cone. This points to the existence of a dominating pressure in the

N.—S. direction in the region of Java—Lesser Sunda Islands, that is released by reverse or thrust faulting if the smallest pressure is in an about vertical direction, and by transcurrent faulting in the case of an under a small angle dipping smallest pressure component. It is remarkable that most of the maximal pressure components with anomalous directions are of the group of very deep earthquakes.

In figure 25 the data are shown of the Philippines arc. The N. Celebes shocks have not been used to exclude the data from a radical other direction of structural lines. An angle α of 30° has been used. There is not much system in the data, but the "tension" components show a preference for N.—NW.—W. to S.—S.E.—E. directions and the pressure components for N.E., vertical and S.W. directions. Most dominating seems to be a tension in a direction of about N.W.—S.E. that is released either by transcurrent faults (with pressure in N.E. and S.W. directions) or by normal faults (in case pressure acts in an about vertical direction).

The New Guinea and Solomon Islands data are given in figure 26 for an angle α of 30°. Also here there is not much system in the distribution of "pressures" and "tensions". On the whole it can be said that pressures are more manifold in about S. and N. directions, and "tensions" in about E. and W. directions. There are, however, many exceptions. It can be seen that the percentage of normal and reverse faulting is very small by the absence of any principle stress components in a vertical direction.

The data of the N. Celebes and Molucca Islands shocks have also been plotted in a diagram. A consistency of the N. Celebes shocks with those of the Java and Lesser Sunda Islands region, and of the Moluccas shocks with those of the Philippines is apparent. These shocks therefore have accordingly been plotted in the diagrams of figures 24 and 25 respectively, using a different notation.

Conclusions

In conclusion the more prominent facts may be summarized as follows:

1. It is very unlikely that the mechanism in the focus of the earthquakes treated here differs appreciably from the assumed "single-couple" theory.
2. The fault motion and the principal earthquake generating stresses are for deep shocks situated in a more or less vertical plane and for shallow shocks in a more or less horizontal plane.
3. The fault motion is generally directed either about perpendicular to, or about parallel with the direction of the geological structures at the surface.
4. The B-axes are generally situated in an about vertical plane through the tectonic structural lines.

5. The fault motions of the very large earthquakes ($M > 7\frac{1}{2}$) show a tendency to be directed in N.N.W.—S.S.E. azimuths independent of the direction of the seismic zone to which the shocks belong.

6. Percentages of combined normal and reverse fault earthquakes are about 25% higher in the "Mediterranean" zones of Sumatra, Sunda arc, Celebes, and the Philippines, than in the "Pacific" zones of the Solomon Islands and New Guinea.

7. In general the positions of the principal stress components of the shocks do not clearly suggest the existence of a common stress field which is the cause of all earthquakes of an individual zone. The Sunda arc is a possible exception to this rule.

8. The geographical distribution of earthquake types is most clearly shown if the area is divided in smaller parts of seismic zones about 2000 km long. The following regions can be distinguished as such:
   a. *Sumatra—Strait Sunda* region where most earthquakes are caused by a horizontal pressure acting in an about N.N.E.—S.S.W. direction.
   b. *Java—Timor* region and
   c. *N. Celebes* region where the earthquakes in general are caused by a horizontal pressure acting in an about N.—S. direction.
   d. *Philippines* region where most earthquakes are caused by a wrench movement of the Pacific Ocean to N. and N.W. relative to the block to the West.
   e. *Solomon Islands* region and
   f. *E. New Guinea* where most earthquakes seem to be caused by a wrench movement of the Pacific Ocean to S.S.E. relative to the blocks south of it.
   g. *W. New Guinea* where the earthquake motions seem to be directed in the same sense as in the Philippines and thus opposite to E. New Guinea and Solomons.
   h. *Moluccas* region where the earthquake fault motion directions are in best accordance with those of the Philippines, but where the earthquake type distribution is in best accord with the New Guinea and Solomon Islands regions.

ACKNOWLEDGEMENTS

Our sincere thanks are due to the Director of the Meteorological and Geophysical Institute, Djakarta, and to the Staff of the Geophysical Department for the facilities given to one of the co-authors in collecting an important part of the data on which this study is based.

We acknowledge with many thanks the readiness with which the Directors of the many seismological observatories all over the world supplied us with the necessary data to complete this study. Without their help and kind co-operation this investigation would not have been possible.

REFERENCES

BÅTH, M. The density ratio at the boundary of the earth's core. Tellus **6,** 408, 1954.

BYERLY, P. and W. STAUDER. — The mechanism at the focus of an earthquake. Earthq. Notes **29,** 17, 1958.

HODGSON, J. H. The null-vector as a guide to regional tectonic patterns. Publ. Dom. Obs., Ottawa, **20,** 369. 1957.

HODGSON, J. H. and W. M. ADAMS. — A study of the inconsistent observations in the fault plane project. Bull. Seism. Soc. Am., **48,** 17, 1958.

HONDA, H. The mechanism of the earthquakes. Publ. Dom. Obs., Ottawa, **20,** 295, 1957.

INGRAM, R. E. and J. H. HODGSON. — Phase change of PP and pP on reflection at a free surface. Bull. Seism. Soc. Am., **46,** 203, 1956.

MCINTYRE, D. B. and J. M. CHRISTIE. — A discussion of "Nature of the faulting in large earthquakes.". Bull. Geol. Soc. Am., **68,** 645, 1957.

RITSEMA, A. R. Pacific and "Mediterranean" earthquake mechanisms. Trans. Am. Geoph. Un., **38,** 349, 1957a.

RITSEMA, A. R. On the use of transverse waves in earthquake mechanism studies. Verhand. **52,** Lemb. Meteor. Geof., Djakarta, 1957b.

RITSEMA, A. R. On the focal mechanism of Southeast Asian earthquakes. Publ. Dom. Obs., Ottawa, **20,** 341, 1957c.

RITSEMA, A. R. (i, Δ) — Curves for bodily seismic waves of any focal depth. Verhand. **54,** Lemb. Meteor. Geof., Djakarta, 1958.

VELDKAMP, J. Mechanism of shallow and intermediate earthquakes in Sumatra, Verhand. Kon. Ned. Geol. Mijnb. Gen., Geol. Ser. **18,** 295, 1957.

VELDKAMP, J. Some Sumatra earthquakes. Ann. di Geof. **12,** 249, 1959.

WILLMORE, P. L. and J. H. HODGSON. — Charts for measuring azimuth and distance and for tracing seismic rays through the earth. Publ. Dom. Obs., Ottawa, **16,** 405, 1955.

Van de reeks MEDEDELINGEN EN VERHANDELINGEN *zijn bij het Staatsdrukkerij- en Uitgeverijbedrijf nog verkrijgbaar de volgende nummers:*

23, 25, 26, 27, 29*b*, 30, 31, 33, 34*a*, 34*b*, 35, 36, 37, 38, 39, 40, 41, 42, 43, 44, 45, 46, 47, 48.

alsmede:

49. A. Labrijn. Het klimaat van Nederland gedurende de laatste twee en een halve eeuw. — The climate of the Netherlands during the last two and a half centuries. 1945. (114 blz. met 6 fig. en 1 kaart) . . . . . f 1,15

50. J. P. M. Woudenberg. Het verband tussen het weer en de opbrengst van wintertarwe in Nederland. — The correlation between weather and yield of wheat in the Netherlands. 1946. (43 blz. met 6 fig.) 0,70

51. S. W. Visser. Weersverwachtingen op langen termijn in Nederland. — Long range weather forecasts in the Netherlands. 1946. (143 blz. met 25 fig.) 2,05

52. R. J. v. d. Linde en J. P. M. Woudenberg. Een methode ter bepaling van de breedte van een schaduw in verband met den tijd van een jaar en de oriëntatie van het beschaduwde object. — A method for determining the daily variation in width of a shadow in connection with the time of the year and the orientation of the overshadowing object. 1946. (6 blz. met 2 fig, en 2 kaarten) 0,40

53. A. Labrijn. Het klimaat van Nederland. Temperatuur, neerslag en wind. — The climate of the Netherlands. Temperature, precipitations and wind. 1946. (71 blz. met 1 kaart) 2,50

54. C. Kramer. Electrische ladingen aan berijpte oppervlakten. — Electric charges on rime-covered surfaces. 1948. (128 blz. met 17 fig. en 1 afb.) 3,00

55. J. J. Post. Statistisch onderzoek naar de samenhang tussen het weer, de grasproductie en de melkaanvoer. — Statistical research on the correlation between the weather, grass production and milk supply. 1949. (119 blz. met 25 fig. en 6 tab.) 3,00

56. R. J. v. d. Linde and J. P. M. Woudenberg. On the microclimatic properties of sheltered areas. The oak-coppice sheltered area. — Over de microklimatologische eigenschappen van beschutte gebieden. Het landschap met eikenhakhoutwallen. 1950. (151 blz. met 52 fig.) 3,00

57. C. Kramer, J. J. Post en W. Wilten. Klimaat en brouwgerstteelt in Nederland. — Climate and growing of malting-barley in the Netherlands. 1952. (149 blz. met 27 fig.) 2,25

58. W. van der Bijl. Toepassing van statistische methoden in de klimatologie. — Applications of statistical methods in climatology. 1952. (197 blz. met 19 fig.) 7,60

59. Tien wetenschappelijke bijdragen, uitgegeven bij het 100-jarig bestaan van het K.N.M.I. — English summary. 1954. (198 blz. met 53 fig.) 12,50

60. C. Kramer. J. J. Post en J. P. M. Woudenberg. Nauwkeurigheid en betrouwbaarheid van temperatuur- en vochtigheidsbepalingen in buitenlucht met behulp van kwikthermometers. 1954. (60 blz. met 11 fig.). 3,50

62. C. Levert. Regens. Een statistische studie. 1954. (246 blz. met 67 fig. en 143 tab.) 10,00

63. P. Groen. On the behaviour of gravity waves in a turbulent medium, with application to the decay and apparent period increase of swell. 1954. (23 blz.) . . 1,50

64. H. M. de Jong. Theoretical aspects of aeronavigation and its application in aviation meteorology. 1956. (124 blz. met 80 fig., 9 krt. en 3 tab.) 4,50

65. J. G. J. Scholte. On seismic waves in a spherical earth. 1956. (55 blz. met 24 fig.) 5,00

66. G. Verploegh. The equivalent velocities for the Beaufort estimates of the wind force at sea. 1956. (38 blz. met 17 tab.) 1,75

67. G. Verploegh. Klimatologische gegevens van de Nederlandse lichtschepen over de periode 1910—1940. Dl. I: Stormstatistieken. — Climatological data of the Netherlands light-vessels over the period 1910 1940. P.I: Statistics of gales. 1956. (68 blz. met tabellen.) . . . . . f 3,50

68. F. H. Schmidt. On the diffusion of stack gases in the atmosphere. 1957. (60 blz., 12 fig. en tab.) 5,00

69. H. P. Berlage. Fluctations of the general atmospheric circulation of more than one year; their nature and prognostic value. 1957 7,50

70. C. Kramer. Berekening van de gemiddelde grootte van de verdamping voor verschillende delen van Nederland volgens de methode van Penman. 1957. (85 blz., fig. en tab.) 7,00

71. H. C. Bijvoet. A new overlay for the determination of the surface wind over sea from surface weather charts. 1957. (35 blz., fig. en tab.) 2,50

72. J. G. J. Scholte. Rayleigh waves in isotropic and anisotropic elastic media. 1958. (43 blz., fig. en tab.) . . . . . 3,—

73. M. P. H. Weenink. A theory and method of calculation of wind effects on sea levels in a partly-enclosed sea, with special application to the southern coast of the North Sea. 1958. (111 blz. met 28 fig. en tab.) . . . . . 8,—

74. H. M. de Jong. Geostrophic flow. Geostrophic approximation in the upper air flow with application to aeronavigation and air trajectories. 1959. (100 blz. met 17 fig., 14 krt. en 2 tab.) . . . . . 5,—

75. S. W. Visser. A new analysis of some features of the 11-year and 27-day cycles in solar activity and their reflection in geophysical phenomena. 1959. (65 blz. met 16 fig. en 12 tab.) 3,50

911944